

Chasing cosmic inflation: constraints for inflationary models and reheating insights

Mario Ballardini^{a,b,c}

^aDipartimento di Fisica e Scienze della Terra, Università degli Studi di Ferrara, via Giuseppe Saragat 1, 44122 Ferrara, Italy

^bINFN, Sezione di Ferrara, via Giuseppe Saragat 1, 44122 Ferrara, Italy

^cINAF/OAS Bologna, via Piero Gobetti 101, 40129 Bologna, Italy

E-mail: mario.ballardini@unife.it

Abstract. We investigate the impact of different choice of prior's range for the reheating epoch on cosmic inflation parameter inference in light of cosmic microwave background (CMB) anisotropy measurements from the *Planck* 2018 legacy release in combination with BICEP/Keck Array 2018 data and additional late-time cosmological observations such as uncalibrated Type Ia Supernovae from the Pantheon catalogue, baryon acoustic oscillations and redshift space distortions from SDSS/BOSS/eBOSS. Here, we explore in particular the implications for the combination of reheating and inflationary-model parameter space considering $R + R^2$ inflation and a broad class of α -attractor and D-brane models. These inflationary models completely cover the n_s - r parameter space allowed by *Planck* and BICEP/Keck data and represent good targets for future CMB and large-scale structure experiments. We perform a Bayesian model comparison of inflationary models, taking into account the reheating uncertainties.

Contents

1	Introduction	1
2	Slow-roll inflation predictions for the primordial power spectra	2
2.1	Effective description of the reheating phase	4
3	Inflationary models and slow-roll dynamics	6
3.1	$R + R^2$ inflation	7
3.2	Cosmological attractors	8
3.3	D-brane inflation	9
4	Analysis and results	10
4.1	Model comparison for inflationary models	12
4.2	Effect of different reheating scenarios	17
5	Conclusions	19
A	Additional tables	24

1 Introduction

Cosmic inflation [1–6] postulates an epoch of nearly exponential expansion in the very early Universe that flattens the spatial geometry and dilutes troublesome pre-inflationary relics. In its simplest realisation, the nearly exponential expansion is driven by a scalar field ϕ , known as *inflaton*, slowly rolling down a sufficiently flat potential $V(\phi)$. During inflation, quantum fluctuations in the scalar field and in the metric are amplified and stretched to density fluctuations and gravitational waves on cosmological scales, respectively.

Measurements of cosmic microwave background (CMB) anisotropies, such as those from the *Planck* satellite [7–12], have significantly contributed to empirical constraints on cosmic inflation. The tight CMB constraints on spatial curvature, isocurvature fluctuations, and primordial non-Gaussianity all agree with expectations from the canonical single-field slow-roll (SFSR) inflationary paradigm.

Inflation also predicts a B-mode pattern in the CMB polarisation [13–17] from inflationary primordial gravitational waves [18–21] that will be hotly pursued by the next-generation CMB experiments [22–26].

The combination of constraints on the scalar spectral index n_s and tensor-to-scalar ratio r can be used to discriminate between different inflation models. The predictions of any model depend on the number of e -folds $N_k \equiv \ln(a_{\text{end}}/a_k)$ between the moment of horizon crossing for a mode with comoving wavenumber k , determined

by $k = aH$, and the end of inflation. Determining the appropriate number of e -folds is necessary to accurately connect the features of the inflationary potential with cosmological observations [27–32].

The duration of the reheating phase is another essential ingredient in comparing theory with measurements. At the end of inflation, the inflaton field loses its energy, eventually initiating the radiation-dominated phase. In the simplest picture, this process is assumed to be instantaneous. In general, the physics of reheating is expected to be more complicated (see, e.g., Ref. [33] for a review), and it is usually described phenomenologically by two parameters: the number $N_{\text{re}} \equiv \ln(a_{\text{re}}/a_{\text{end}})$ of e -folds between the end of inflation and the beginning of the radiation phase, and \bar{w}_{re} , the average equation-of-state parameter during the reheating phase. Our imprecise knowledge of the physics of reheating introduces uncertainty into the derivation of constraints on the inflationary potential from measurements of n_s and r , dubbed as *reheating uncertainties* [29]. However, there are prospects for using observations to constrain reheating, particularly to constrain the reheating temperature, when all the energy of the inflaton field is converted to radiation [7, 9, 34–38]. Constraining the reheating temperature enables the testing and selection of inflation models with future CMB experiments [39].

More precisely, constraints on reheating are derived by requiring that the number of e -folds between the time that the current comoving horizon scale exited the horizon during inflation and the end of inflation must be related to the number of e -folds between the end of inflation and today. By imposing this requirement, several groups have derived constraints on the reheating parameter space and the inflationary-potential parameter space for various SFSR inflation models [40–46]; these constraints have been obtained mainly using measurements of the scalar spectral index.

In this paper, we update the *Planck* inflationary analysis [11] including the latest BICEP/Keck data [47] focusing to a broader range of α -attractor and D-brane inflationary models. We focus on the impact of different assumptions on the reheating phase and on the constraints on the reheating parameters derived from current cosmological observations.

This paper is organised as follows. In Section 2, we review the computational method adopted to describe the primordial power spectra of scalar and tensor fluctuations for a given SFSR inflationary model. We also review the derivation of the number of e -folds, taking into account the uncertainties connected to an effective description of the reheating phase. We introduce the selection of inflationary models that we will study and their basic equations used for the analysis in Section 3. We present and discuss our results in Section 4 for all the models analysed and for different parametrisation choice of reheating scenario. We conclude in Section 5.

2 Slow-roll inflation predictions for the primordial power spectra

For a SFSR inflationary model, starting from the action given by

$$S = \int d^4x \sqrt{-g} \left[\frac{M_{\text{Pl}}^2 R}{2} - \frac{1}{2} \partial_\mu \phi \partial^\mu \phi - V(\phi) \right], \quad (2.1)$$

the dynamical equations for the background, namely the Friedmann equation and the Klein-Gordon equation, are respectively

$$H^2 = \frac{1}{3M_{\text{Pl}}^2} \left(\frac{\dot{\phi}}{2} + V \right), \quad (2.2a)$$

$$\ddot{\phi} + 3H\dot{\phi} + V_\phi = 0, \quad (2.2b)$$

where $V_\phi \equiv dV/d\phi$ and the background metric is the flat Friedmann-Robertson-Walker one given by $ds^2 = -dt^2 + a^2(t)dx^2 = a^2(t)(-d\tau^2 + dx^2)$. At leading order in perturbations, the equation of motion in term of gauge-invariant quantity is given by [48]

$$v_{\mathbf{k}}'' + \left[k^2 - \frac{(a\sqrt{\epsilon_1})''}{a\sqrt{\epsilon_1}} \right] v_{\mathbf{k}} = 0 \quad (2.3)$$

for scalar perturbations and for tensor perturbations

$$v_{\mathbf{k}}'' + \left[k^2 - \frac{a''}{a} \right] v_{\mathbf{k}} = 0. \quad (2.4)$$

Primordial power spectra (PPS) of scalar and tensor cosmological fluctuations can be described with an analytic perturbative expansion. The result is an unified framework to connect the predictions for hundreds of slow-roll inflationary models to cosmological observations [49, 50].

The method, developed in Ref. [18] for tensor perturbations and in Refs. [51, 52] for scalar perturbations, has been improved and extended including higher-order corrections at next-to-leading order (NLO) in Refs. [53–57], and next-next-to-leading (NNLO) in Refs. [58, 59]. Using the calculation based on the Green's function method [55], the PPS for scalar (S) and tensor (T) perturbations can be expanded in terms of $\ln k$, around a particular reference scale k_* up to NLO [57], giving

$$\ln \frac{P_X(k)}{P_{X0}(k_*)} = b_{X0} + b_{X1} \ln \left(\frac{k}{k_*} \right) + \frac{1}{2} b_{X2} \ln^2 \left(\frac{k}{k_*} \right) + \dots, \quad (2.5)$$

where $X = \{S, T\}$ and the normalisation of the PPS are given by

$$P_{S0} = \frac{H_*^2}{8\pi^2 M_{\text{Pl}}^2 \epsilon_1}, \quad P_{T0} = \frac{2H_*^2}{\pi^2 M_{\text{Pl}}^2}. \quad (2.6)$$

The expansion coefficients, up to NLO of Hubble flow functions (HFF) ϵ_n , are given by

$$\begin{aligned} b_{S0} = & -2(1 - \alpha)\epsilon_1 + \alpha\epsilon_2 + \left(2\alpha + \frac{\pi^2}{2} - 5 \right) \epsilon_1^2 \\ & + \left(-\alpha^2 + 3\alpha + \frac{7\pi^2}{12} - 6 \right) \epsilon_1\epsilon_2 + \left(\frac{\pi^2}{8} - 1 \right) \epsilon_2^2 \\ & + \left(-\frac{\alpha^2}{2} + \frac{\pi^2}{24} \right) \epsilon_2\epsilon_3, \end{aligned} \quad (2.7a)$$

$$b_{S1} = -2\epsilon_1 - \epsilon_2 - 2\epsilon_1^2 - (3 - 2\alpha)\epsilon_1\epsilon_2 - \alpha\epsilon_2\epsilon_3, \quad (2.7b)$$

$$b_{S2} = -2\epsilon_1\epsilon_2 - \epsilon_2\epsilon_3, \quad (2.7c)$$

for scalar perturbations, and

$$b_{\text{T0}} = -2(1 - \alpha)\epsilon_1 + \left(2\alpha + \frac{\pi^2}{2} - \frac{10}{2}\right)\epsilon_1^2 + \left(-\alpha^2 + 2\alpha + \frac{\pi^2}{12} - 2\right)\epsilon_1\epsilon_2, \quad (2.8a)$$

$$b_{\text{T1}} = -2\epsilon_1 - 2\epsilon_1^2 - 2(1 - \alpha)\epsilon_1\epsilon_2, \quad (2.8b)$$

$$b_{\text{T2}} = -2\epsilon_1\epsilon_2, \quad (2.8c)$$

for tensor perturbations. Here $\alpha \equiv \gamma_{\text{E}} + \ln(2) - 2 \approx 0.7296$ and γ_{E} is the Euler-Mascheroni constant. The needed HFF to describe the NLO expansion are

$$\epsilon_1 = 2M_{\text{Pl}}^2 \left(\frac{H'}{H}\right)^2, \quad (2.9a)$$

$$\epsilon_2 = 4M_{\text{Pl}}^2 \left[\left(\frac{H'}{H}\right)^2 - \frac{H''}{H} \right], \quad (2.9b)$$

$$\epsilon_3 = 2M_{\text{Pl}}^2 \left[2 \left(\frac{H'}{H}\right)^2 + \frac{H'''}{H'} - 3 \frac{H''}{H} \right] \left(1 - \frac{HH''}{H'^2}\right)^{-1}, \quad (2.9c)$$

where a prime ' denotes derivative with respect to conformal time τ . HFF can be calculated directly from a given single-field potential [54] as

$$\epsilon_1 \simeq \frac{M_{\text{Pl}}^2}{2} \left(\frac{V_\phi}{V}\right)^2, \quad (2.10a)$$

$$\epsilon_2 \simeq 2M_{\text{Pl}}^2 \left[\left(\frac{V_\phi}{V}\right)^2 - \frac{V_{\phi\phi}}{V} \right], \quad (2.10b)$$

$$\epsilon_2\epsilon_3 \simeq 2M_{\text{Pl}}^4 \left[\frac{V_{\phi\phi\phi}V_\phi}{V^2} - 3 \frac{V_{\phi\phi}}{V} \left(\frac{V_\phi}{V}\right)^2 + 2 \left(\frac{V_\phi}{V}\right)^4 \right]. \quad (2.10c)$$

2.1 Effective description of the reheating phase

In order to derive accurate predictions, we need to calculate the number of e -folds from the time that a given perturbation scale leaves the horizon until the end of inflation. This requires knowledge about the end of inflation, how the Universe reheats, and the post-inflationary evolution of the Universe, for a given model; see Refs. [27, 28, 30].

We can expand the definition of comoving Hubble scale $k = a_k H_k$ evaluated at the time of horizon exit such that

$$\frac{k}{a_0 H_0} = \frac{a_k}{a_{\text{end}}} \frac{a_{\text{end}}}{a_{\text{re}}} \frac{a_{\text{re}}}{a_{\text{eq}}} \frac{H_k}{H_{\text{eq}}} \frac{a_{\text{eq}} H_{\text{eq}}}{a_0 H_0}. \quad (2.11)$$

The number of e -folds between the time at which the comoving wavenumber k crossing the comoving Hubble radius and the end of inflation is defined as $e^{N_k} \equiv a_{\text{end}}/a_k$. The

number of e -folds between the end of inflation and the beginning of the radiation-dominated phase, dubbed as *reheating phase*, is $e^{N_{\text{re}}} \equiv a_{\text{re}}/a_{\text{end}}$. The duration of reheating can be described through an effective average equation of state

$$\begin{aligned}\rho_{\text{re}} &= \rho_{\text{end}} e^{3 \int \frac{da}{a} [1+w_{\text{re}}(a)]} \\ &= \rho_{\text{end}} e^{3 \int_{N_{\text{end}}}^N dN' [1+w_{\text{re}}(N')]} \\ &= \rho_{\text{end}} e^{-3N_{\text{re}}(1+\bar{w}_{\text{re}})},\end{aligned}\tag{2.12}$$

where the final energy density during reheating can be expressed as

$$\rho_{\text{re}} = \frac{\pi^2}{30} g_{\text{re}} T_{\text{re}}^4,\tag{2.13}$$

with g_{re} being the effective number of relativistic species upon thermalisation. Combining Eq. (2.13) and Eq. (2.12), we can express the reheating temperature as

$$T_{\text{re}} = \frac{30\rho_{\text{end}}}{\pi^2 g_{\text{re}}} e^{-3N_{\text{re}}(1+\bar{w}_{\text{re}})}.\tag{2.14}$$

The reheating temperature can be related to the CMB temperature today T_γ assuming that the reheating entropy is conserved in the CMB and neutrino background today, that corresponds to entropy conservation $d(sa^3) = 0$. This gives

$$a_{\text{re}}^3 g_{\text{s, re}} T_{\text{re}}^3 = a_0^3 \left(2 + \frac{7}{8} 2 \frac{4}{11} N_{\text{eff}} \right) T_\gamma^3,\tag{2.15}$$

where $g_{\text{s, re}}$ is the effective number of relativistic degrees of freedom for entropy at the end of reheating and we assumed that neutrino temperature today is given by $T_\nu = (4/11)^{1/3} T_\gamma$. Combining Eq. (2.14) with Eq. (2.15), we obtain

$$\frac{a_{\text{re}}}{a_0} = \left(2 + \frac{7}{11} N_{\text{eff}} \right)^{1/3} T_\gamma \frac{g_{\text{re}}^{1/4}}{g_{\text{s, re}}^{1/3}} \left(\frac{\pi^2}{30\rho_{\text{end}}} \right)^{1/4} e^{\frac{3}{4} N_{\text{re}}(1+\bar{w}_{\text{re}})}.\tag{2.16}$$

The last term of Eq. (2.11) can be calculated from the Friedmann equation in the form

$$\frac{H_{\text{eq}}}{H_0} = \sqrt{(1+z_{\text{eq}})^4 \Omega_\gamma + (1+z_{\text{eq}})^3 \Omega_{\text{m}} + \Omega_\Lambda} = 218.65 (1+z_{\text{eq}}) \Omega_{\text{m}} h,\tag{2.17}$$

where we assumed a spatially-flat background with $\Omega_k = 0$. We obtain for the number of e -folds between horizon crossing and the end of inflation

$$N_k = 67.27 - \ln \left(\frac{k}{a_0 H_0} \right) - \frac{1}{12} \ln \left(\frac{g_{\text{s, re}}^4}{g_{\text{re}}^3} \right) - \frac{1-3\bar{w}_{\text{re}}}{4} N_{\text{re}} + \frac{1}{4} \ln \left(\frac{H_k^4}{\rho_{\text{end}}} \right).\tag{2.18}$$

We split the last term on the right hand side separating the dependence from the end of inflation to the one at the horizon crossing as

$$\frac{1}{4} \ln \left(\frac{H_k^4}{\rho_{\text{end}}} \right) = \frac{1}{4} \ln \left(\frac{V_k}{3 - \epsilon_{1, k}} \frac{3 - \epsilon_{1, \text{end}}}{3V_{\text{end}}} \right) + \frac{1}{4} \ln (8\pi^2 A_{\text{s}} \epsilon_{1, k}),\tag{2.19}$$

where $A_s \equiv P_{S0}(k_*)$. Inserting in Eq. (2.18), we obtain

$$\begin{aligned}
N_k &= 66.72 - \ln\left(\frac{k}{a_0 H_0}\right) \\
&\quad - \frac{1}{12} \ln\left(\frac{g_{s,\text{re}}^4}{g_{\text{re}}^3}\right) - \frac{1 - 3\bar{w}_{\text{re}}}{4} N_{\text{re}} \\
&\quad + \frac{1}{4} \ln\left(\frac{3V_k \epsilon_{1,k}}{3 - \epsilon_{1,k}} \frac{3 - \epsilon_{1,\text{end}}}{V_{\text{end}}}\right) + \frac{1}{4} \ln(8\pi^2 A_s). \tag{2.20}
\end{aligned}$$

Using Eq. (2.12), we can rewrite the number of e -folds during reheating as

$$N_{\text{re}} = -\frac{1}{3 + 3\bar{w}_{\text{re}}} \ln\left(\frac{\rho_{\text{re}}}{\rho_{\text{end}}}\right). \tag{2.21}$$

Eq. (2.20) allows for an accurate value for the number of e -folds between horizon crossing and the end of inflation. We fix the values of the cosmological parameters to $N_{\text{eff}} = 3.044$ [60], $T_\gamma = 2.7255$ K [61], $H_0 = 67.36$ km s⁻¹ Mpc⁻¹, and $\Omega_m = 0.3153$ [62], the pivot scale to $k_* = 0.05$ Mpc⁻¹. It is reasonable to assume all the particles to be in thermal equilibrium in the early Universe, that corresponds to $g_{\text{re}} = g_{s,\text{re}}$, and we fix $g_{\text{re}} = 106.75$ to the Standard Model (SM) prediction even if a larger value for g_{re} might arise at high energies in beyond SM theories.

Finally, the most convenient way to write the number of e -folds is

$$\begin{aligned}
N_{0.05} &= 60.9 + \frac{1 - 3\bar{w}_{\text{re}}}{12 + 12\bar{w}_{\text{re}}} \ln\left(\frac{\rho_{\text{re}}}{M_{\text{Pl}}^4}\right) + \frac{1 + 3\bar{w}_{\text{re}}}{6 + 6\bar{w}_{\text{re}}} \ln(8\pi^2 A_s) \\
&\quad + \frac{1}{3 + 3\bar{w}_{\text{re}}} \ln\left[\frac{V_*}{V_{\text{end}}} \frac{2}{3 - \epsilon_{1,*}} (3\epsilon_{1,*})^{\frac{1+3\bar{w}_{\text{re}}}{2}}\right], \tag{2.22}
\end{aligned}$$

where we consider as parameters $\ln(\rho_{\text{re}}/M_{\text{Pl}}^4)$, A_s , \bar{w}_{re} (hereafter we will simple use w_{re} for the effective average equation of state during reheating), and $\epsilon_{1,\text{end}} = 1$.

3 Inflationary models and slow-roll dynamics

For single-field inflationary models with a standard kinetic term and a potential $V(\phi)$, we can calculate analytically the PPS of scalar and tensor fluctuations given a shape of inflationary potential combining Eq. (2.7) and Eq. (2.8) with Eq. (2.10). Finally, in order to have expressions in terms of the number of e -folds rather than values of the scalar field, we need to solve the expression of the classical inflationary trajectory

$$N_* \equiv N_{\text{end}} - N_* = -\frac{1}{M_{\text{Pl}}^2} \int_{\phi_*}^{\phi_{\text{end}}} d\phi \frac{V}{V_\phi}. \tag{3.1}$$

In the following, we will provide the expression of the inflationary trajectory $\phi(N)$ and for the value of the field at which inflation end ϕ_{end} , such that $\epsilon_{1,\text{end}} \equiv \epsilon_1(\phi_{\text{end}}) = 1$, for each of the inflationary models studied.

3.1 $R + R^2$ inflation

The first inflationary model proposed in Ref. [1] is based on higher-order gravitational terms as

$$\frac{\mathcal{L}}{\sqrt{-g}} = \frac{1}{2} \left(R + \frac{R^2}{6M^2} \right). \quad (3.2)$$

In the conformally-related Einstein frame (EF), it corresponds to a scalar field ϕ with potential

$$V_{R+R^2}(\phi) = V_0 \left(1 - e^{-\sqrt{\frac{2}{3}}\phi} \right)^2. \quad (3.3)$$

The condition $\epsilon_{1,\text{end}} = 1$ occurs for

$$\phi_{\text{end}} = \sqrt{\frac{3}{2}} \ln \left(1 + \frac{2}{\sqrt{3}} \right), \quad (3.4)$$

and the slow-roll trajectory can be expressed inverting Eq. (3.1) as

$$\begin{aligned} \phi_* = \sqrt{\frac{3}{2}} \left\{ -\frac{4}{3}N_* - \left(1 + \frac{2}{\sqrt{3}} \right) + \ln \left(1 + \frac{2}{\sqrt{3}} \right) \right. \\ \left. - W_{-1} \left[-e^{-\frac{4}{3}N_* - \left(1 + \frac{2}{\sqrt{3}} \right) + \ln \left(1 + \frac{2}{\sqrt{3}} \right)} \right] \right\}, \end{aligned} \quad (3.5)$$

where W_{-1} is the Lambert function in the -1 -branch.

We can now derive predictions for the scalar spectral index n_s and the tensor-to-scalar ratio r calculating Eq. (2.10) with Eq. (3.3) and Eq. (3.5). The leading-order predictions in the limit $N \gg 1$ [48, 63] are

$$n_s \approx 1 - \frac{2}{N}, \quad r \approx \frac{12}{N^2}. \quad (3.6)$$

The same predictions come from a scalar field model with $V(\phi) = \lambda\phi^4/4$ at large values of ϕ and a large non-minimal coupling to gravity $\xi R\phi^2$, including the Higgs inflation model [64].

Solving Eq. (2.22) for the number of e -folds at horizon crossing one finds $N_{0.05} \simeq 54.8$ for instantaneous reheating, that corresponds to $N_{\text{re}} = 0$, and $N_{0.05} \simeq 50.3$ for $T_{\text{re}} = 3.1 \times 10^9$ GeV [65, 66] assuming that the Universe is in a matter-dominated stage while the scalaron decays into the SM Higgs bosons [1, 67]. It is important to stress that while for these values leading-order predictions (3.6) lead to

$$n_s(N_{0.05} \simeq 54.8) = 0.9635, \quad r(N_{0.05} \simeq 54.8) = 0.0040, \quad (3.7)$$

$$n_s(N_{0.05} \simeq 50.3) = 0.9602, \quad r(N_{0.05} \simeq 50.3) = 0.0047, \quad (3.8)$$

using second-order slow-roll analytic predictions gives

$$n_s(N_{0.05} \simeq 54.8) = 0.9653, \quad r(N_{0.05} \simeq 54.8) = 0.0034, \quad (3.9a)$$

$$n_s(N_{0.05} \simeq 50.3) = 0.9623, \quad r(N_{0.05} \simeq 50.3) = 0.0040, \quad (3.9b)$$

resulting in a 15% difference.

3.2 Cosmological attractors

Many cosmological attractor models have been proposed to make the inflationary predictions of simple scalar fields compatible with cosmological data generalising their kinetic term. Two simple examples of α -attractors [68–73] are given by

$$\frac{\mathcal{L}}{\sqrt{-g}} = \frac{R}{2} - \frac{1}{2} \frac{(\partial_\mu \phi)^2}{\left(1 - \frac{\phi^2}{6\alpha}\right)^2} - V(\phi), \quad (3.10)$$

the so called T-model, and the E-model

$$\frac{\mathcal{L}}{\sqrt{-g}} = \frac{R}{2} - \frac{3\alpha}{4} \frac{(\partial_\mu \phi)^2}{\phi^2} - V(\phi). \quad (3.11)$$

α -attractors represent a special class of pole inflation models [73], described by the equation

$$\frac{\mathcal{L}}{\sqrt{-g}} = \frac{R}{2} - \frac{a_q}{2} \frac{(\partial_\mu \phi)^2}{\phi^q} - V(\phi), \quad (3.12)$$

where $q = 2$, $a_2 = 3\alpha/2$ reduces to the E-models of α -attractors.¹ The origin of the pole in the kinetic term can be explained in the context of hyperbolic geometry in supergravity and string theory [75], or related to a non-minimal coupling of the inflaton field to gravity [68, 73, 76]. Using a canonical normalised scalar field φ , it is possible to rewrite the theory as

$$\frac{\mathcal{L}}{\sqrt{-g}} = \frac{R}{2} - \frac{(\partial_\mu \varphi)^2}{2} - V(\varphi), \quad (3.13)$$

where the potential and its derivatives are not singular. For the simplest case $V(\phi) \propto \phi^{2n}$, in terms of the canonical variables, we have

$$V_{\text{T-model}}(\varphi) = V_0 \tanh^{2n} \left(\frac{\varphi}{\sqrt{6\alpha}} \right), \quad (3.14)$$

and

$$V_{\text{E-model}}(\varphi) = V_0 \left(1 - e^{-\sqrt{\frac{2}{3\alpha}} \varphi} \right)^{2n}. \quad (3.15)$$

In case of $n = 1$, Eq. (3.15) corresponds to the EF potential in the $R + R^2$ inflation [18] and Higgs inflation [64] for $\alpha = 1$, and Goncharov-Linde (GL) model of chaotic inflation in supergravity [77] for $\alpha = 1/9$. The case of $\alpha = 2$, $n = 1/2$ corresponds to fibre inflation [78, 79].

The condition $\epsilon_{1,\text{end}} = 1$ for T-model and E-model occurs for

$$\varphi_{\text{end}}^{\text{T}} = \sqrt{\frac{3\alpha}{2}} \sinh^{-1} \left(\frac{2n}{\sqrt{3\alpha}} \right), \quad (3.16)$$

$$\varphi_{\text{end}}^{\text{E}} = \sqrt{\frac{3\alpha}{2}} \ln \left(\frac{2n}{\sqrt{3\alpha}} + 1 \right), \quad (3.17)$$

¹See Ref. [74] for previously introduced T-model and the E-model conformal attractors.

and the slow-roll trajectories can be expressed as

$$\varphi_*^{\text{T}} = \sqrt{\frac{3\alpha}{2}} \operatorname{sech}^{-1} \left(\frac{3\alpha}{\alpha \sqrt{\frac{12n^2}{\alpha} + 9} + 4nN_*} \right), \quad (3.18)$$

$$\varphi_*^{\text{E}} = \sqrt{\frac{3\alpha}{2}} \left\{ -\frac{4n}{3\alpha} N_* - \left(1 + \frac{2n}{\sqrt{3\alpha}} \right) + \ln \left(1 + \frac{2n}{\sqrt{3\alpha}} \right) - W_{-1} \left[-e^{-\frac{4n}{3\alpha} N_* - \left(1 + \frac{2n}{\sqrt{3\alpha}} \right) + \ln \left(1 + \frac{2n}{\sqrt{3\alpha}} \right)} \right] \right\}. \quad (3.19)$$

The predictions of the T-models (3.14) coincide with the ones of the E-models (3.15) in the limits for $\alpha \rightarrow 0$ and $\alpha \rightarrow \infty$. For $\alpha \gg 1$, the model predictions correspond to the ones for large-field chaotic models $V(\varphi) \propto \varphi^{2n}$ [6], while for $\alpha \ll 1$ to

$$n_s \approx 1 - \frac{2}{N}, \quad r \approx \frac{12\alpha}{N^2} \quad (3.20)$$

for both T-models and E-models and for all values n . For $\alpha < 1$, α -attractors predict a value of the tensor-to-scalar ratio smaller than the one predicted in $R + R^2$ inflation.

3.3 D-brane inflation

String theory D-brane inflation models [80–83] correspond to Dp-brane- $\overline{\text{D}p}$ -brane interaction where the inflationary potentials have the form

$$V_{\text{BI}}(\phi) = V_0 \left[1 - \left(\frac{m}{\phi} \right)^{7-p} + \dots \right], \quad (3.21)$$

in brane inflation, and

$$V_{\text{KKLT}}(\phi) = V_0 \left[1 + \left(\frac{m}{\phi} \right)^{7-p} \right]^{-1}, \quad (3.22)$$

in Kachru-Kalosh-Linde-Trivedi (KKLT) inflation [84]. Models well compatible with cosmological observations are the inverse quadratic (D5- $\overline{\text{D}5}$) and inverse quartic (D3- $\overline{\text{D}3}$) [85, 86], both associated with type IIB string theory and possible moduli stabilisation due to KKLT [84] and LVT [87, 88] construction. In addition, the inverse linear case with D6- $\overline{\text{D}6}$ potential in type IIA string theory [89, 90]. In this case

$${}^1V_{\text{BI}}(\phi) = V_0 \left(1 - \frac{m}{|\phi|} + \dots \right), \quad (3.23)$$

and

$${}^1V_{\text{KKLT}}(\phi) = V_0 \left(1 + \frac{m}{|\phi|} \right)^{-1}, \quad (3.24)$$

where ϕ is a distance in the moduli space. Brane inflation potential (3.21) is unbounded from below and it requires a consistent generalisation, in particular for the parameter

space region allowed by data, that is $\phi < m$. The predictions of (3.21) coincide with the one of (3.22) in the limit for $\phi < m$.

For the KKLТ potential there is no generic solution for ϕ_{end} . Analytical solutions can be found for integer values of p or for the limits $\phi \ll m$ and $\phi \gg m$.

Similarly to α -attractors, KKLТ models have universal predictions for $m \lesssim 1$ and small r . In this limit, we have

$${}^4n_s \approx 1 - \frac{5}{3N}, \quad {}^2n_s \approx 1 - \frac{3}{2N}, \quad {}^1n_s \approx 1 - \frac{4}{3N} \quad (3.25)$$

corresponding to the same predictions of n_s for $V(\phi) \propto \phi^{2n}$ with $n = \frac{7-p}{9-p}$, and

$${}^4r \approx \frac{4m^{4/3}}{(3N)^{5/3}}, \quad {}^2r \approx \frac{12m}{N^2}, \quad {}^1r \approx \frac{8m^{2/3}}{(3N)^{3/4}}. \quad (3.26)$$

4 Analysis and results

We use `CosmoMC` [91] connected to our modified version of the code `CAMB` [92, 93] sampled with the nested sampling code `PolyChord` [94, 95], which allow to obtain simultaneously the log-evidence. Mean values and uncertainties on the parameters, as well as the posterior distributions plotted, have been generated using `GetDist` [96]. For the computation of the Kullback-Leibler (KL) divergence, we rely on `anesthetic` [97].

We use *Planck* temperature, polarisation, and lensing 2018 legacy PR3 data [98] (hereafter P18). Low-multipole data for $\ell < 30$ consists to the `commander` likelihood for temperature and `SimAll` for the E-mode polarisation. On high multipoles $\ell \geq 30$, we use the `Plik` likelihood including CMB temperature up to $\ell_{\text{max}} = 2508$, E-mode polarisation and temperature-polarisation cross correlation up to $\ell_{\text{max}} = 1996$. We include B-mode polarisation spectrum for $20 < \ell < 330$ from BICEP2, Keck Array, and BICEP3 observations up to 2018 [47] (hereafter BK18). Additionally, we include measurements of baryon acoustic oscillations (BAO) and redshift space distortions (RSD) at low redshift $0.07 < z < 0.2$ from SDSS-I and -II sample as *Main Galaxy Sample* (MGS), BOSS DR12 galaxies over the redshift interval $0.2 < z < 0.6$, eBOSS luminous red galaxies (LRG) and quasars $0.6 < z < 2.2$, and Lyman- α forest samples $1.8 < z < 3.5$ [99]. We also include the Pantheon catalogue of uncalibrated Type Ia Supernovae (SNe) over the redshift range $0.01 < z < 2.3$ [100].

In addition to the inflationary parameters discussed in the previous section, we vary the standard cosmological parameters ω_b , ω_c , θ_{MC} , τ , A_s , as well as nuisance and foreground parameters. As baseline, we allow the reheating phase to last down to $\rho_{\text{re}}^{1/4} = 1 \text{ TeV}$ maximum and to happen in a matter-dominated phase, corresponding to $w_{\text{re}} = 0$.² We will present in the next section results for different assumptions on the reheating phase. Prior ranges on the standard and inflationary parameters are

²For inflationary potentials that can be approximated to $V(\phi) \propto \phi^{2n}$ around their minima, after inflation, the homogeneous inflaton field oscillates initially with average equation of state given by $\bar{w}_{\text{hom}} = (n-1)/(n+1)$ [101].

Parameter	Uniform prior
$\omega_b \equiv \Omega_b h^2$	[0.019, 0.025]
$\omega_c \equiv \Omega_c h^2$	[0.095, 0.145]
$100\theta_{\text{MC}}$	[1.03, 1.05]
τ	[0.01, 0.4]
$\ln(10^{10} A_s)$	[2.5, 3.7]
$\ln(\rho_{\text{re}}/M_{\text{Pl}}^4)$	$[\ln(1 \text{ TeV}/M_{\text{Pl}}^4), \ln(\rho_{\text{end}}/M_{\text{Pl}}^4)]$
$\log \alpha^{\text{T}}$	[-2, 4]
$\log \alpha^{\text{E}}$	[-2, 4]
$\log m$	[-4, 4]

Table 1. Prior ranges for cosmological parameters used in the Bayesian comparison of inflationary models.

Model	$N_{0.05}$	$n_{s,0.05}$	$r_{0.05}$
$R + R^2$	[45, 55]	[0.958, 0.966]	[0.0034, 0.0049]
T-model $n = 1/2$	[44, 56]	[0.955, 0.973]	$[3 \times 10^{-5}, 0.086]$
T-model $n = 2/3$	[44, 56]	[0.955, 0.971]	$[4 \times 10^{-5}, 0.11]$
T-model $n = 1$	[44, 57]	[0.955, 0.964]	$[4 \times 10^{-5}, 0.17]$
T-model $n = 3/2$	[44, 57]	[0.947, 0.964]	$[4 \times 10^{-5}, 0.25]$
GL	[44, 54]	[0.957, 0.964]	$[4.3 \times 10^{-4}, 6.2 \times 10^{-4}]$
Poincaré	[45, 55]	[0.959, 0.966]	[0.007, 0.010]
E-model $n = 1/2$	[44, 56]	[0.955, 0.973]	$[4 \times 10^{-5}, 0.080]$
E-model $n = 2/3$	[44, 56]	[0.955, 0.971]	$[4 \times 10^{-5}, 0.11]$
E-model $n = 1$	[44, 57]	[0.949, 0.964]	$[4 \times 10^{-5}, 0.16]$
E-model $n = 3/2$	[44, 57]	[0.949, 0.963]	$[4 \times 10^{-5}, 0.23]$
KKLT $p = 3$	[42, 58]	[0.937, 0.968]	$[4 \times 10^{-9}, 0.32]$
KKLT $p = 5$	[43, 57]	[0.957, 0.972]	$[3 \times 10^{-7}, 0.17]$
KKLT $p = 6$	[44, 56]	[0.967, 0.976]	$[2 \times 10^{-5}, 0.09]$

Table 2. Allowed ranges for some derived inflationary parameters taking into account Eq. (2.22) and propagating the dependence on the variation of α for α -attractors and m for KKLT inflation, respectively.

collected on Table 1. We report a rough estimation of the allowed prior ranges for some derived parameters in Table 2. Note that α -attractors can easily describe any value of $r \ll 1$ without spoiling the predictions on the scalar spectral index. In Table 2, the lower value for the tensor-to-scalar ratio reflects the prior range adopted on the parameter α , sufficiently large for the sensitivity of current CMB measurements.

Theoretical predictions for the scalar spectral index and the tensor-to-scalar ratio at $k_* = 0.05 \text{ Mpc}^{-1}$ are shown in Fig. 1 for the range of parameters considered in the analysis given in Table 1 and in Table 2.

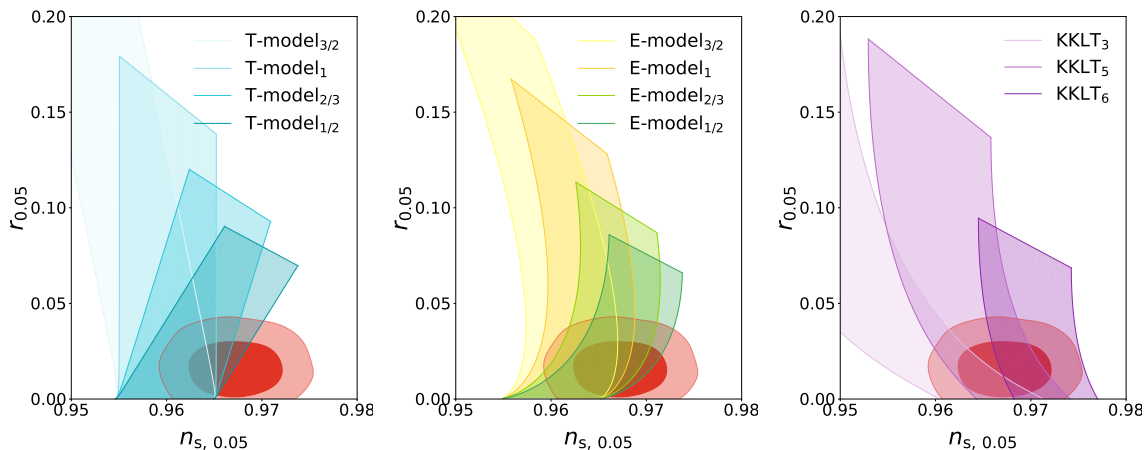


Figure 1. Marginalised joint confidence contours for the scalar spectral index $n_{s,0.05}$ and tensor-to-scalar ratio $r_{0.05}$ for the Λ CDM+ r model at 68% CL and 95% CL compared to the theoretical predictions for T-model α -attractor (left panel), E-model α -attractor (central panel), and KKLT (right panel) inflation.

4.1 Model comparison for inflationary models

We perform a Bayesian analysis of the combination of datasets described above given the model parameters, including the reheating uncertainties. Here we sample directly on the inflationary parameters rather than sampling on slow-roll parameters ϵ_n or the phenomenological ones ($n_s, \alpha_s, n_t, \dots$) to describe the shape of the PPS. We have zero extra parameters for $R + R^2$ inflation (synonymous of Starobinsky inflation) and for GL inflation (E-model with $n = 1$ and $\alpha^E = 1/9$) while one extra parameter for the other inflationary models considered. We have α_n^T for T-model α -attractor, α_n^E for E-model α -attractor, and m_p for KKLT inflation.

All the results are presented in comparison to the flat Λ CDM+ r model to highlight the differences on the posterior distributions of n_s and r , that are derived parameters in our cases. This shows that the results are dominated by theoretical prior knowledge on the models injected in the analysis.

In Fig. 2, we show the 68% CL and 95% CL posterior distributions of the scalar spectral index $n_{s,0.05}$ and tensor-to-scalar ratio $r_{0.05}$ for $R + R^2$ inflation, T-model and E-model of α -attractor inflation for $n = 1/2, 2/3, 1, 3/2$, and KKLT inflation for $p = 3, 5, 6$, for the baseline reheating scenario. We collect constraints and mean values on the inflationary parameters in Table 3.

$R + R^2$ marginalised posterior distributions are well in agreement with the reference posteriors obtained for the phenomenological power-law case with a predicted value of the scalar spectral index slightly lower than the 68% CL; see Fig. 2. The predictions in the basic version of the $R + R^2$ (corresponding to the star in Fig. 2) gives a smaller value of the scalar spectral index compared to α -attractors. The reason is that in the basic $R + R^2$ model the only interactions are gravitational, and therefore reheating is inefficient, which leads to a smaller number of e -folds and consequently a smaller scalar spectral index. For comparison, reheating in the Higgs inflation is very

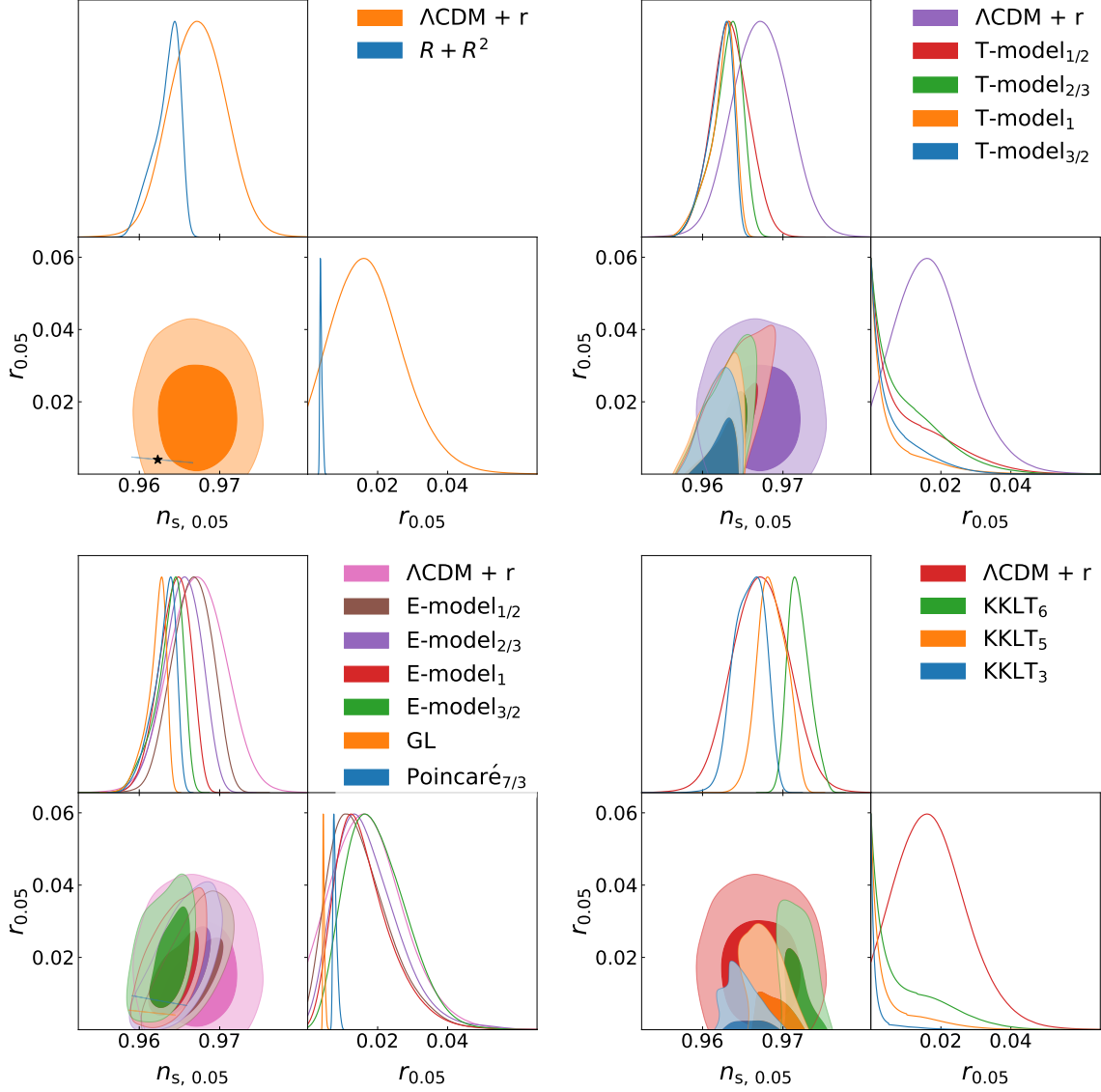


Figure 2. Marginalised joint confidence contours for the scalar spectral index $n_{s,0.05}$ and tensor-to-scalar ratio $r_{0.05}$ for $R + R^2$ inflation (upper left), T-model of α -attractor inflation (upper right), E-model of α -attractor inflation (lower left), and KKLT inflation (lower right), at 68% CL and 95% CL. In the E-model panel we include the contours for GL inflation corresponding to $n = 1$ and $\alpha = 1/9$ [77, 102] and for Poincaré disk inflation with $n = 1$ and $\alpha^E = 7/3$ [103, 104]. Here reheating parameters correspond to $w_{\text{re}} = 0$ and $\rho_{\text{re}}^{1/4} > 1 \text{ TeV}$. The star in the upper left panel corresponds to the standard prediction in $R + R^2$ inflation assuming the values for reheating from [65, 66].

Parameter	Λ CDM+ r	$R + R^2$	GL	Poincaré $_{7/3}$
$\ln(10^{10} A_s)$	$3.048^{+0.012}_{-0.014}$	3.048 ± 0.012	3.046 ± 0.013	3.049 ± 0.014
$\ln(\rho_{\text{re}}/M_{\text{Pl}}^4)$ (at 95% CL)	–	> -118	> -91.5	> -106
$n_{s,0.05}$	0.9672 ± 0.0035	$0.9634^{+0.0021}_{-0.0011}$	$0.9621^{+0.0015}_{-0.0007}$	$0.9630^{+0.0018}_{-0.0009}$
$r_{0.05}$ (at 95% CL)	< 0.036	$0.0038^{+0.0002}_{-0.0004}$	$0.0046^{+0.0002}_{-0.0003}$	$0.0078^{+0.0013}_{-0.0009}$
$N_{0.05}$	–	$52.0^{+3.0}_{-1.6}$	$53.1^{+2.1}_{-1.1}$	$52.7^{+2.6}_{-1.4}$
$\log(T_{\text{re}}/\text{GeV})$ (at 95% CL)	–	> 5.0	> 7.8	> 6.2

Parameter	T-model $_{1/2}$	T-model $_{2/3}$	T-model $_1$	T-model $_{3/2}$
$\ln(10^{10} A_s)$	$3.047^{+0.012}_{-0.013}$	3.051 ± 0.013	3.047 ± 0.014	3.049 ± 0.013
$\ln(\rho_{\text{re}}/M_{\text{Pl}}^4)$ (at 95% CL)	> -118	> -113	> -113	> -108
α^{T} (at 95% CL)	< 14.7	< 10.6	< 7.3	< 6.3
$n_{s,0.05}$	0.9635 ± 0.0023	$0.9630^{+0.0023}_{-0.0014}$	$0.9624^{+0.0020}_{-0.0010}$	$0.9622^{+0.0019}_{-0.0011}$
$r_{0.05}$ (at 95% CL)	< 0.034	< 0.030	< 0.024	< 0.023
$N_{0.05}$	$51.9^{+2.9}_{-1.9}$	$52.3^{+2.8}_{-1.6}$	$52.2^{+2.8}_{-1.5}$	$52.3^{+2.7}_{-1.7}$
$\log(T_{\text{re}}/\text{GeV})$ (at 95% CL)	> 5.0	> 5.5	> 5.5	> 6.0

Parameter	E-model $_{1/2}$	E-model $_{2/3}$	E-model $_1$	E-model $_{3/2}$
$\ln(10^{10} A_s)$	3.051 ± 0.013	3.050 ± 0.014	3.049 ± 0.014	3.049 ± 0.013
$\ln(\rho_{\text{re}}/M_{\text{Pl}}^4)$ (at 95% CL)	–	–	> -108	> -108
α^{E} (at 95% CL)	< 30.9	< 25.9	< 16.8	< 16.1
$n_{s,0.05}$	$0.9666^{+0.0027}_{-0.0023}$	$0.9654^{+0.0026}_{-0.0021}$	$0.9643^{+0.0022}_{-0.0017}$	$0.9637^{+0.0021}_{-0.0011}$
$r_{0.05}$ (at 95% CL)	< 0.032	$0.017^{+0.018}_{-0.016}$	$0.016^{+0.017}_{-0.014}$	$0.020^{+0.017}_{-0.015}$
$N_{0.05}$	$51.8^{+3.2}_{-2.0}$	$51.6^{+3.0}_{-2.2}$	$52.7^{+2.7}_{-1.6}$	$53.3^{+2.6}_{-1.3}$
$\log(T_{\text{re}}/\text{GeV})$ (at 95% CL)	–	–	> 5.8	> 6.1

Parameter	KKLT $_3$	KKLT $_5$	KKLT $_6$
$\ln(10^{10} A_s)$	$3.057^{+0.012}_{-0.014}$	3.056 ± 0.013	$3.055^{+0.015}_{-0.017}$
$\ln(\rho_{\text{re}}/M_{\text{Pl}}^4)$ (at 95% CL)	–	–	< -42.6
$m [M_{\text{Pl}}]$ (at 95% CL)	< 5.6	< 5.1	< 6.8
$n_{s,0.05}$	$0.9659^{+0.0021}_{-0.0017}$	0.9687 ± 0.0018	$0.9720^{+0.0011}_{-0.0016}$
$r_{0.05}$ (at 95% CL)	< 0.011	< 0.023	< 0.030
$N_{0.05}$	$49.1^{+2.6}_{-3.1}$	$48.9^{+2.4}_{-3.4}$	$48.6^{+1.7}_{-3.2}$
$\log(T_{\text{re}}/\text{GeV})$ (at 95% CL)	–	–	< 13.1

Table 3. Constraints on the main and derived parameters (at 68% CL if not otherwise stated) for Λ CDM+ r , $R + R^2$, GL, Poincaré, α -attractor inflation, and KKLT inflation considering the combination P18+BK18+BAO+RSD+SNe.

efficient, leading to a larger value of the scalar spectral index [66].

α -attractor inflation and KKLT inflation cover a larger portion of the n_s - r parameter space than the extra parameter. While the latter covers better the left part of the contour plot, the former covers larger values of the scalar spectral index. E-model α -attractor inflation is able to fit the hint of non-zero primordial gravitational waves in BK18 observations with a value of the scalar spectral index compatible to the other cosmological datasets (mostly driven by P18 data).

While we consider α as a continuous parameter in our analysis, there are examples, such as in advanced supergravity models, where α assumes discrete values; see Refs. [103, 104]. These values correspond to $3\alpha = 7, 6, 5, 4, 3, 2, 1$ and the associated models are usually called Poincaré disk models. We consider a specific case of Poincaré disk inflation with $n = 1$ and $\alpha^E = 7/3$, with zero extra parameters as $R + R^2$ and GL inflation; see Fig. 2 and Table 3.

The reheating energy density parameter $\ln(\rho_{\text{re}}/M_{\text{Pl}}^4)$ is often unconstrained since all the inflationary models considered here are well in agreement with cosmological observations as can be seen in Figs. 4 and 5 (dotted lines). Indeed, there is no need of a specific reheating behaviour to accommodate their predictions. However, there is a preference for a short reheating period for $R + R^2$ and α -attractor inflation while a longer period seems preferred for KKLT inflation; see Figs. 4 and 5.

For α -attractor and KKLT inflation the constraints on the additional inflationary parameter correspond roughly to $\alpha^T \lesssim 20$, $\alpha^E \lesssim 30$, and $m/M_{\text{Pl}} \lesssim 10$ at 95% CL, see Table 3.

We investigate the log-evidence and KL divergence for the inflationary model analysed in comparison to the $\Lambda\text{CDM}+r$ model [44, 46]. We calculate the evidence $\mathcal{Z} \equiv P(\mathcal{D}|\mathcal{M})$, that is the marginal likelihood for the model \mathcal{M} , and we report the Bayes' factors as

$$\Delta \ln \mathcal{Z} = \ln \frac{P(\mathcal{D}|\mathcal{M})}{P(\mathcal{D}|\mathcal{M}_{\Lambda\text{CDM}+r})}, \quad (4.1)$$

where the evidence is given by

$$\mathcal{Z} \equiv P(\mathcal{D}|\mathcal{M}) = \int d\theta P(\mathcal{D}|\theta, \mathcal{M})\pi(\theta). \quad (4.2)$$

and $\Delta \log \mathcal{Z} > 0$ favours the reference model, here the $\Lambda\text{CDM}+r$. $P(\mathcal{D}|\theta, \mathcal{M})$ is the likelihood of the parameters θ given the data \mathcal{D} . In order to quantify going from the prior distribution to the posterior distribution, we calculated the relative entropy or KL divergence

$$\mathcal{D}_{\text{KL}} = \int d\theta P(\theta|\mathcal{D}, \mathcal{M}) \ln \left(\frac{P(\theta|\mathcal{D}, \mathcal{M})}{\pi(\theta)} \right) \quad (4.3)$$

where $P(\theta|\mathcal{D}, \mathcal{M})$ is the posterior distribution of the parameters θ and $\pi(\theta)$ are the prior ranges on the parameters. We show these quantities in Fig. 3 in a triangle plot, for all the inflationary models analysed. See Refs. [44, 46, 50] for an extended discussion on KL divergence and other Bayesian estimators in the context of inflationary models.

Looking at the relative log-evidence, we can see a clear preference for the inflationary models studied compared to the $\Lambda\text{CDM}+r$ model. The inflationary models that

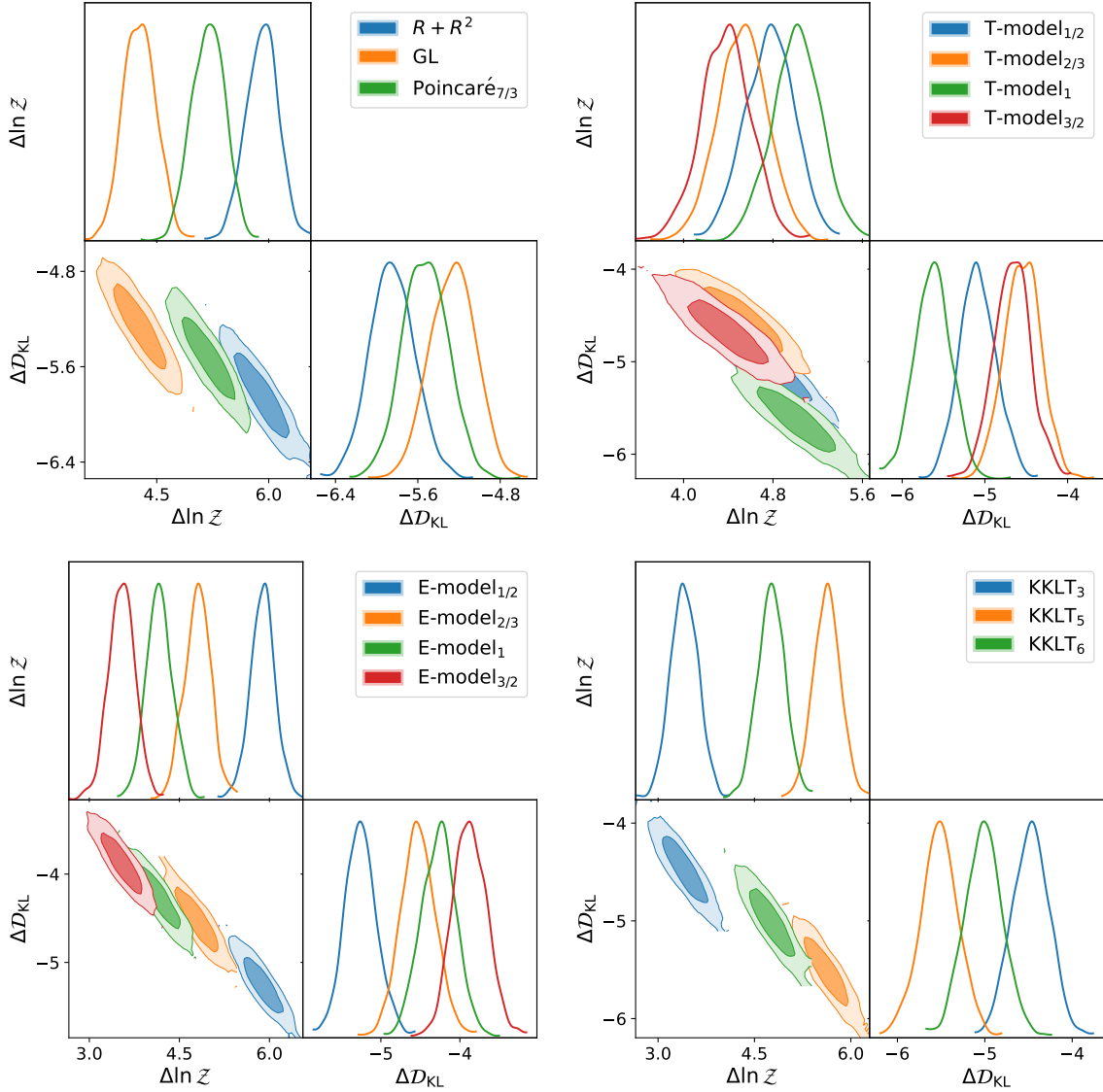


Figure 3. Relative log-evidence $\Delta \ln \mathcal{Z}$ and relative KL divergence $\Delta \mathcal{D}_{\text{KL}}$ for the $R+R^2$, GL, Poincaré disk, α -attractor, and KKLT inflation with respect to $\Lambda\text{CDM}+r$ assuming baseline reheating scenario.

perform better for each class are $R+R^2$ inflation with $\Delta \ln \mathcal{Z} = 5.9 \pm 0.2$, T-model α -attractor inflation for $n = 1$ with $\Delta \ln \mathcal{Z} = 5.0 \pm 0.2$, E-model α -attractor inflation for $n = 1/2$ with $\Delta \ln \mathcal{Z} = 5.9 \pm 0.2$, and KKLT inflation for $p = 5$ with $\Delta \ln \mathcal{Z} = 5.6 \pm 0.2$. Comparing the different models no one results preferred according to the revised Jeffrey’s scale [105]; we always have for any pair of inflationary models $\Delta \ln \mathcal{Z} < 2.5$. This estimator tends to penalise the addition of parameters which usually leads to spread the model’s predictive probability over a larger parameter space. Here, $R+R^2$, GL, and Poincaré disk inflation have six cosmological parameters, α -attractor and KKLT inflation seven parameters, and the reference $\Lambda\text{CDM}+r$ seven as well. Note that, the

inclusion of the tensor-to-scalar ratio, with prior range of $r_{0.05} \in [0, 1]$, penalises the reference model compared to the standard Λ CDM model without primordial tensors which on the other hand would be preferred as discussed in Ref. [44, 106]. Moreover, the scalar spectral index and the tensor-to-scalar ratio are derived parameters for the inflationary models in our analysis leading to an unavoidable use of different prior which might affect the model comparison, see Refs. [44, 46].

In terms of relative KL divergence, we can see no prior-to-posterior distribution compression for the inflationary model parameters. Indeed, while in Λ CDM+ r all the cosmological parameters are well constrained for the given prior ranges with a tight upper bound for the tensor-to-scalar ratio, for the inflationary models the reheating parameters are often unconstrained by current cosmological data.

4.2 Effect of different reheating scenarios

In this section, we compare the baseline reheating scenario studied in the previous subsection, in which the reheating phase last down to $\rho_{\text{re}}^{1/4} = 1 \text{ TeV}$ maximum and with $w_{\text{re}} = 0$, to the following two reheating scenarios:

restrictive $\rho_{\text{re}}^{1/4} > 1 \text{ TeV}$, $-1/3 < w_{\text{re}} < 1/3$,

permissive $\rho_{\text{re}}^{1/4} > 10 \text{ MeV}$, $-1/3 < w_{\text{re}} < 1$.³

Here the energy density is bounded by requiring the reheating phase to end before electroweak scale ($\sim 10^2 \text{ GeV}$) in the restrictive case and before Big Bang nucleosynthesis happens ($\sim 1 \text{ MeV}$) [107] in the permissive case.

Different reheating scenarios affect the inflationary predictions leading to different number of e -folds between horizon crossing and the end of inflation according to Eq. (2.18). The baseline reheating scenario studied in the previous subsection with $\rho_{\text{re}}^{1/4} > 1 \text{ TeV}$ and $w_{\text{re}} = 0$ corresponds to $\Delta N \simeq -11.8$ maximum with respect to assume instantaneous reheating. Indeed, in the baseline reheating scenario we can have less e -folds compared to the assumption of instantaneous reheating. For $w_{\text{reh}} = 0$, assuming a larger prior for the reheating energy density, as in the permissive case, corresponds to additional $\Delta N \simeq -3.8$ e -folds going from 1 TeV to 10 MeV. For $w_{\text{reh}} \neq 0$ the situation is a bit more convolved. In the restrictive case, the prefactor $(1 - 3w_{\text{re}})/(12 + 12w_{\text{re}})$, which multiply N_{re} , can vary in the range $[0, 0.25]$. For $-1/3 < w_{\text{re}} < 0$, we can have even less e -folds compared to the baseline case while keeping fix the reheating energy density. For $0 < w_{\text{re}} < 1/3$ the impact of the reheating uncertainties on the inflationary predictions is reduced compared to the baseline case. In the permissive case, for $1/3 < w_{\text{re}} < 1$, the prefactor changes sign leading in this case to a larger number of e -folds compared to instantaneous reheating.

In Figs. 4 and 5 the posterior distributions of the effective equation of state parameter w_{re} (for the restrictive and permissive reheating), the energy density at the end of reheating $\ln(\rho_{\text{re}}/M_{\text{pl}}^4)$ (for the baseline, the restrictive, and the permissive reheating), and the number of e -folds $N_{0.05}$ between the scale $k_* = 0.05 \text{ Mpc}^{-1}$ crosses

³Similar and additional choices have been considered in Refs. [7, 46].

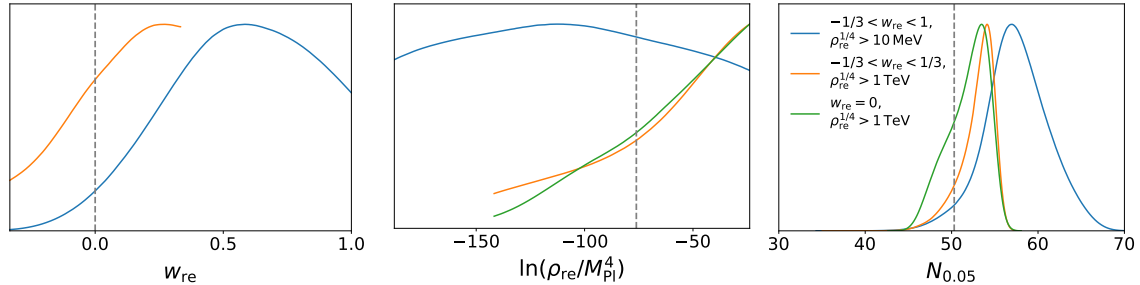


Figure 4. Posterior distribution in $R + R^2$ inflation for the effective equation of state parameter w_{re} (left panel), the energy density at the end of reheating $\ln(\rho_{\text{re}}/M_{\text{pl}}^4)$ (central panel), and the number of e -folds between the scale k_* crosses the horizon and the end of inflation $N_{0.05}$ (right panel) for the minimal ($w_{\text{re}} = 0$, $\rho_{\text{re}}^{1/4} > 1 \text{ TeV}$), restricted ($-1/3 < w_{\text{re}} < 1/3$, $\rho_{\text{re}}^{1/4} > 1 \text{ TeV}$), and permissive ($-1/3 < w_{\text{re}} < 1$, $\rho_{\text{re}}^{1/4} > 10 \text{ MeV}$) reheating scenario in blue, orange, and green, respectively. The dashed vertical lines correspond to the standard value for reheating in $R + R^2$ inflation from [65, 66].

the horizon and the end of inflation (for the baseline, the restrictive, and the permissive reheating) are shown; see Tables 4 and 5 for means and uncertainties on the inflationary parameters assuming restrictive and permissive reheating scenarios, respectively.

We find that the results for $R + R^2$ and α -attractor inflation with the restrictive reheating scenario are close to the ones obtained fixing $w_{\text{re}} = 0$; see Figs. 6 and 7. For these models a short reheating period is enough to fit cosmological observations. Moreover, these models would need a larger value of e -folds to be able to fit a larger value of the scalar spectral index. The situation is different for KKLТ inflation where a longer reheating period is preferred in order to compensate for the higher value of the scalar spectral index predicted; see Fig. 8. Moving to the permissive reheating scenario all α -attractor and KKLТ models are able to cover the whole allowed n_s - r parameter space; this is mostly driven by the larger prior on w_{re} .⁴ Results for $R + R^2$ inflation do not change much since inflationary predictions are bounded to run only along the constrain equation $r \approx 3(1 - n_s)^2$; the model has no extra parameters to relax this relation.

Finally, we derive also the constraints on the temperature at the end of reheating using Eq. (2.13). As for the reheating energy density, this parameter result often unconstrained with current cosmological data, see Tables 4 and 5. Note that, supersymmetric theories, such as those associated with α -attractors, are affected by the *gravitino problem*. To avoid this problem, it is crucial to restrict the reheating temperature to higher than 10^9 GeV to prevent the overproduction of gravitinos [45, 109]. This lower bound, compatible with our findings, can be used to further tighten the prior ranges of the model inflationary parameters.

⁴Note that the range $1/3 < w_{\text{re}} < 1$ is less plausible but possible, see Ref. [108].

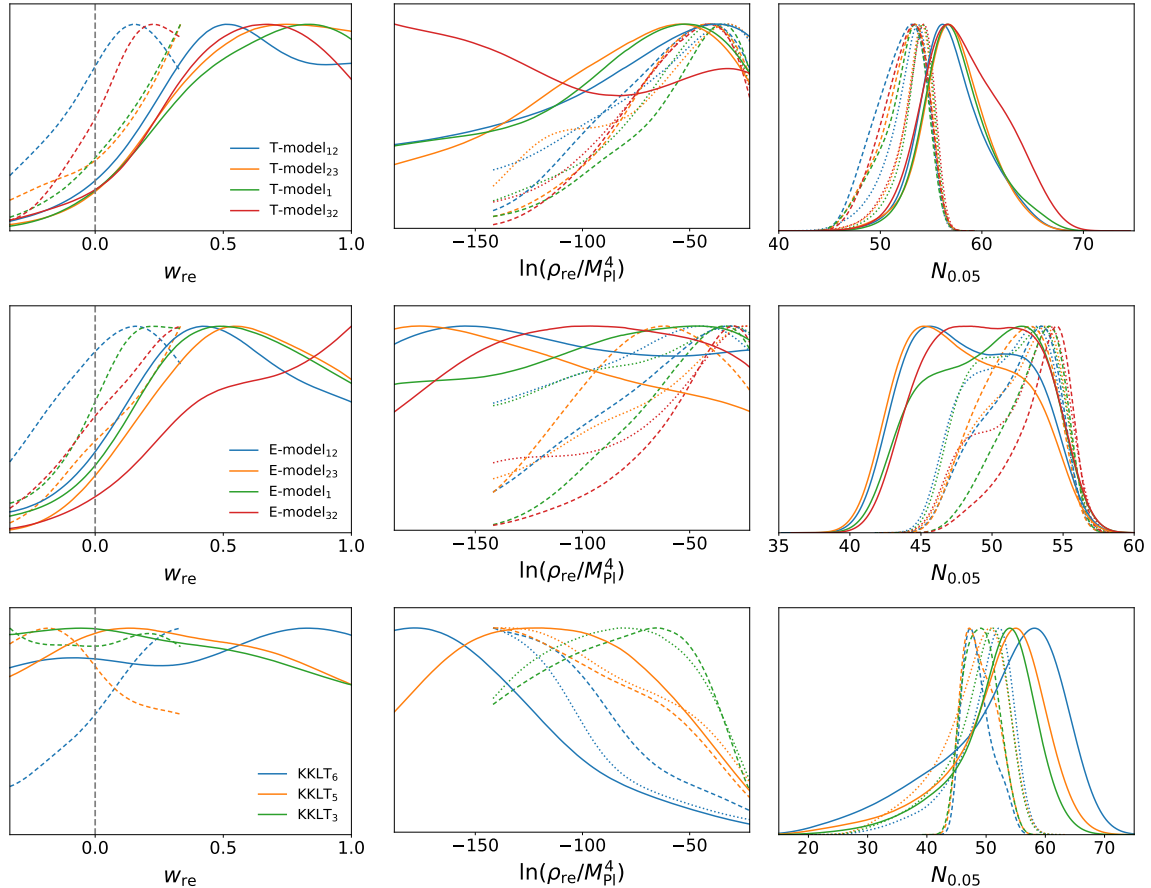


Figure 5. Same as Fig. 4 for T-model of α -attractor inflation (upper row), E-model of α -attractor inflation (central row), and KKLT inflation (lower row). Solid lines correspond to the permissive reheating scenario, dashed ones to the restricted reheating scenario, and the dotted ones to our baseline reheating scenario.

5 Conclusions

The recent advancements in precision cosmology, particularly driven from the *Planck* legacy data [11] and new upper limits on B-modes from BICEP/Keck [47], represent a significant step forward in refining constraints on inflationary models.⁵ Predictions for inflationary parameters, such as the scalar spectral index and the tensor-to-scalar ratio, are intricately linked through consistency relations, offering valuable insights into the dynamics of early Universe expansion.

Looking ahead, the next decade will likely see improvements primarily in the precision of constraints on the scalar spectral index and the tensor-to-scalar ratio. Expectations for future measurements suggest a potential threefold improvement in the error bars of the scalar spectral index n_s at best from ground-based CMB experiment, such as Simons Observatory and CMB-S4 [24, 25], and from their combination with

⁵See Refs. [110–112] for analysis based on the combination of BICEP/Keck data and post-legacy reanalysis of *Planck* data, namely the *Planck* PR4 [113, 114].

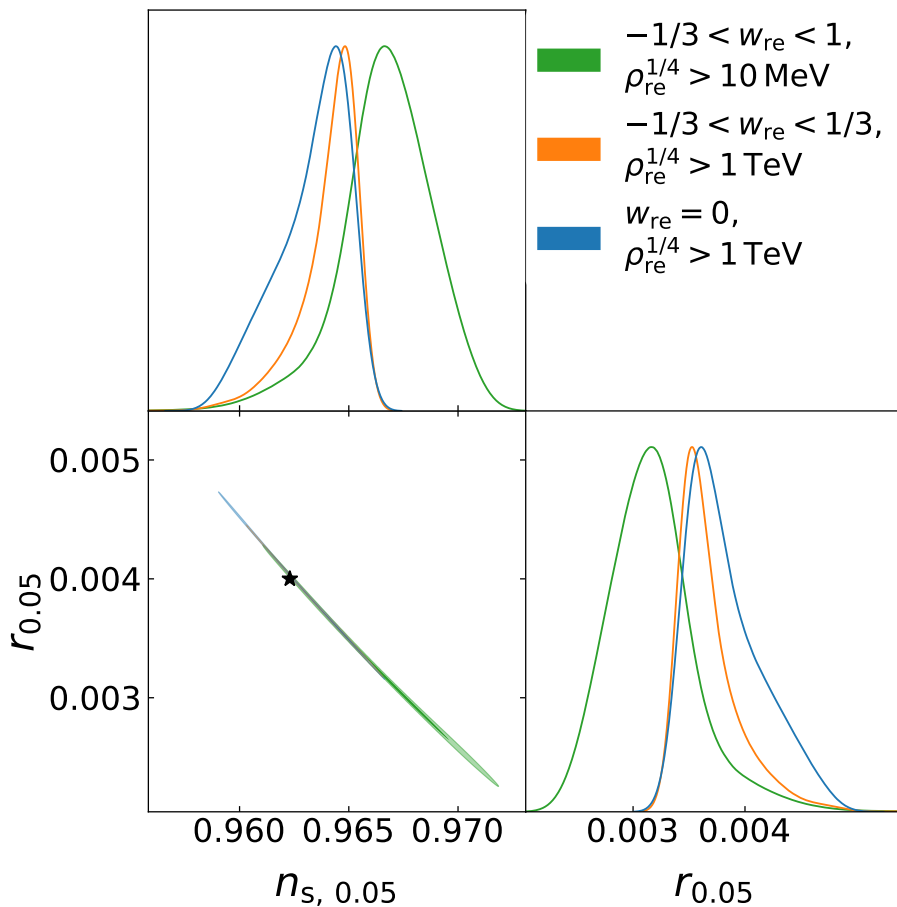


Figure 6. Marginalised joint confidence contours for the scalar spectral index $n_{s,0.05}$ and tensor-to-scalar ratio $r_{0.05}$ for $R + R^2$ inflation at 68% CL and 95% CL for the baseline ($w_{\text{re}} = 0$, $\rho_{\text{re}}^{1/4} > 1 \text{ TeV}$), restricted ($-1/3 < w_{\text{re}} < 1/3$, $\rho_{\text{re}}^{1/4} > 1 \text{ TeV}$), and permissive ($-1/3 < w_{\text{re}} < 1$, $\rho_{\text{re}}^{1/4} > 10 \text{ MeV}$) reheating scenario in blue, orange, and green, respectively. Here reheating parameters correspond to $w_{\text{re}} = 0$ and $\rho_{\text{re}}^{1/4} > 1 \text{ TeV}$. The star corresponds to the prediction standard in $R + R^2$ inflation assuming standard values for reheating from [65, 66].

large-scale structures experiments such as *Euclid* [115–117]. Conversely, advancements in B-mode polarisation measurements in the CMB anisotropies [23], such as those expected from the LiteBIRD satellite [26], hold promise for significantly constraining the tensor-to-scalar ratio r , potentially by several orders of magnitude [24–26].

In our study, we investigated the implications of recent BICEP/Keck measurements in combination to *Planck*'s ones for a selection of inflationary models, including $R + R^2$, α -attractor, and D-brane inflation models. The models considered completely cover the n_s - r parameter space allowed by *Planck* and BICEP/Keck data all the way down to $r = 0$ [118], resulting also as good candidates to be targeted by future CMB experiments [104, 119]. By deriving the scalar spectral index and the tensor-to-scalar ratio up to second order in slow-roll and considering reheating uncertainties, we pro-

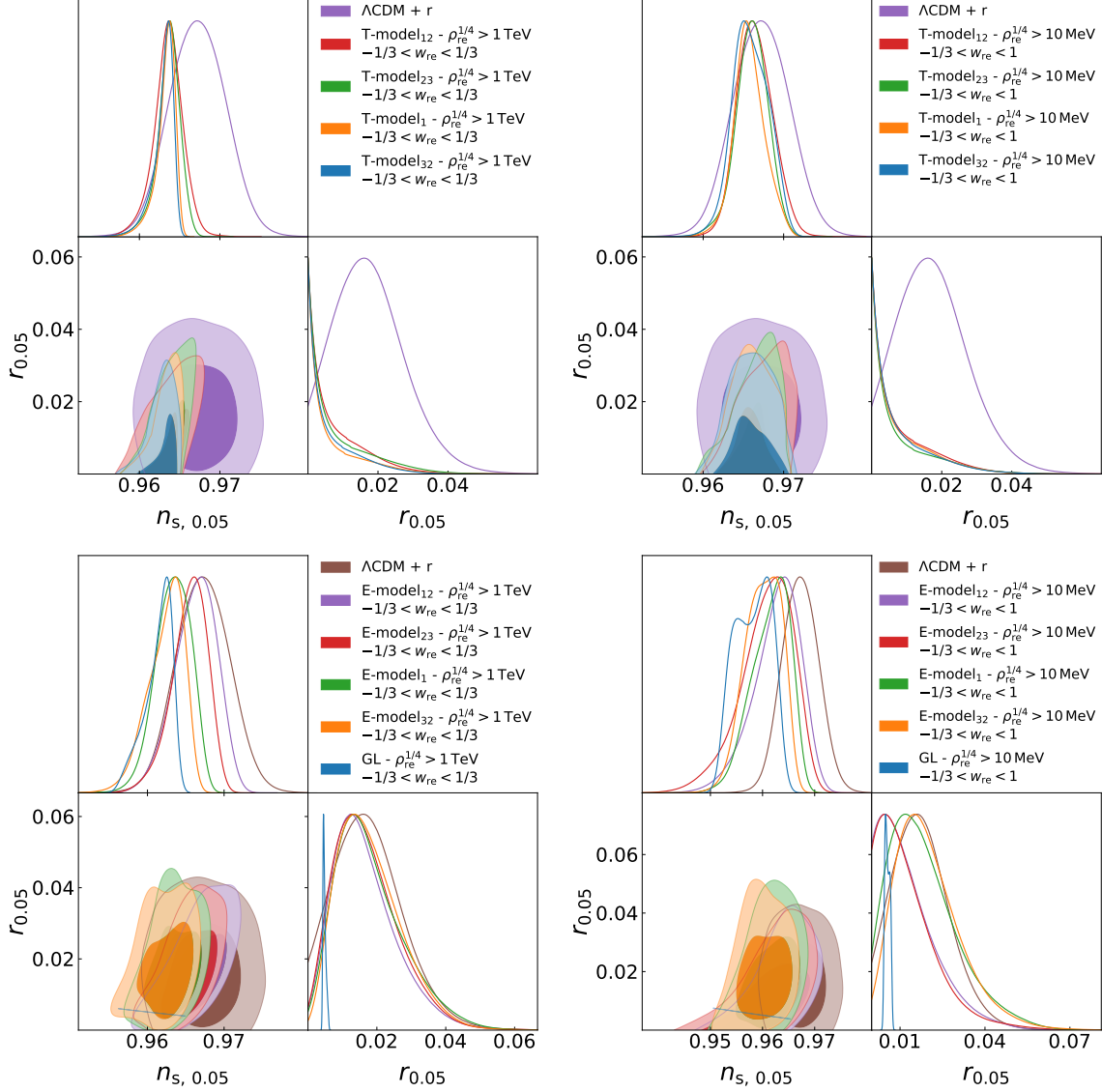


Figure 7. Marginalised joint confidence contours for the scalar spectral index $n_{s,0.05}$ and tensor-to-scalar ratio $r_{0.05}$ for T-model (top panels) and for E-model (bottom panels) of α -attractor inflation at 68% CL and 95% CL for the restrictive reheating scenario on the left ($-1/3 < w_{\text{re}} < 1/3$, $\rho_{\text{re}}^{1/4} > 1 \text{ TeV}$) and the permissive reheating one on the right ($-1/3 < w_{\text{re}} < 1$, $\rho_{\text{re}}^{1/4} > 10 \text{ MeV}$).

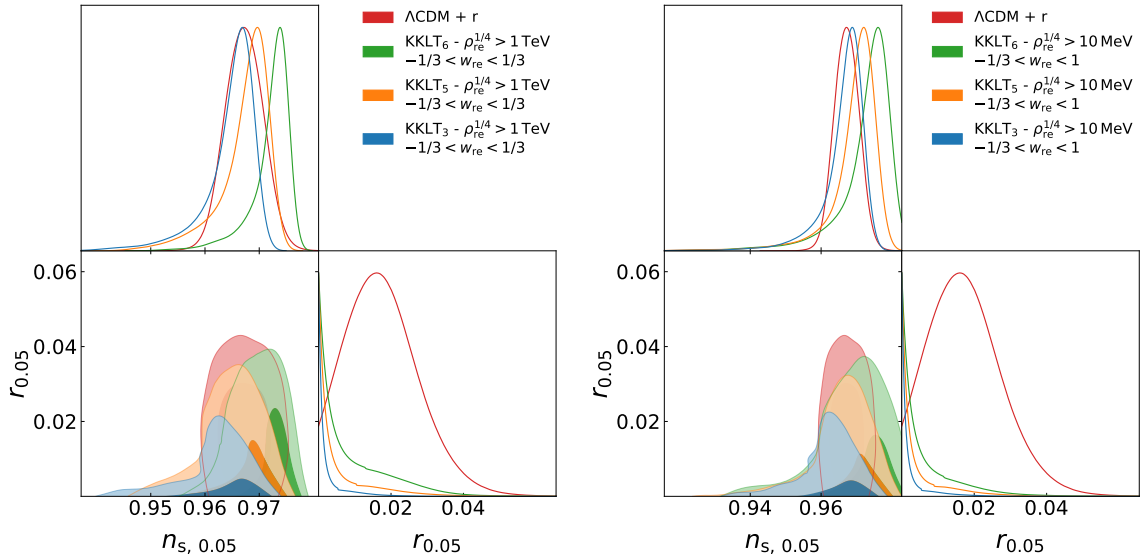


Figure 8. Same as Fig. 7 for KKLT inflation.

vided insights into the compatibility of these models with CMB observations.

Our analysis revealed the importance of combined constraints on n_s and r to disentangle different inflationary models as well as the importance to include the theoretical information on the reheating phase to shrink the predicted parameter space. Indeed, reheating uncertainties and uncertainties on inflationary parameters can be further reduced injecting in the analysis the information on the energy density distribution and equation of state of the universe between the end of inflation and the onset of radiation domination based on numerical simulations of the reheating epoch [120–122].

Of course, one should remember that exact predictions of these models not only depend on details of the models and mechanism of reheating, the addition of different datasets can shift (mostly along the n_s direction) the position of the allowed region [123]. For instance, the addition of recent DESI DR1 galaxy and quasar BAO to *Planck* data leads to a higher value of the scalar spectral index $n_s = 0.9700 \pm 0.0036$ at 68% CL [124, 125], eventually going in the direction of preferring D-brane inflationary models, while ACT DR4 data points to even larger values as $n_s = 1.008 \pm 0.015$ at 68% CL [126].

In conclusion, if future measurements align with the current maximum likelihood values for r , and if inflation proceeded through a single-field slow-roll mechanism, detecting non-zero values for the running of spectral indexes and tensor spectral indexes may pose a challenge to the prevailing inflationary paradigm. Continued advancements in B-mode measurements are expected to provide further insights into the inflationary parameter space.

Acknowledgments

The author is grateful to Andrei Linde and Renata Kallosh for useful comments. I acknowledge financial support from the INFN InDark initiative and from the COSMOS network (www.cosmosnet.it) through the ASI (Italian Space Agency) Grants 2016-24-H.0, 2016-24-H.1-2018, 2020-9-HH.0 (participation in LiteBIRD phase A). I also acknowledge financial support by “Bando Giovani anno 2023 per progetti di ricerca finanziati con il contributo 5x1000 anno 2021”.

Parameter	Λ CDM+ r	$R + R^2$	GL	Poincaré $_{7/3}$
$\ln(10^{10} A_s)$	$3.048^{+0.012}_{-0.014}$	$3.050^{+0.012}_{-0.014}$	$3.049^{+0.012}_{-0.013}$	3.049 ± 0.013
$\ln(\rho_{\text{re}}/M_{\text{Pl}}^4)$ (at 95% CL)	–	–	–	–
w_{re} (at 95% CL)	–	–	–	> -0.22
$n_{s, 0.05}$	0.9672 ± 0.0035	$0.9641^{+0.0015}_{-0.0007}$	$0.9612^{+0.0026}_{-0.0013}$	$0.9625^{+0.0024}_{-0.0012}$
$r_{0.05}$ (at 95% CL)	< 0.036	$0.0037^{+0.0006}_{-0.0004}$	$0.0048^{+0.0011}_{-0.0007}$	$0.0081^{+0.0016}_{-0.0012}$
$N_{0.05}$	–	$53.0^{+2.3}_{-1.0}$	$51.9^{+3.5}_{-1.9}$	$51.9^{+3.3}_{-1.9}$
$\log(T_{\text{re}}/\text{GeV})$ (at 95% CL)	–	–	> 4.0	–

Parameter	T-model $_{1/2}$	T-model $_{2/3}$	T-model $_1$	T-model $_{3/2}$
$\ln(10^{10} A_s)$	3.050 ± 0.012	$3.054^{+0.013}_{-0.016}$	3.049 ± 0.013	$3.050^{+0.013}_{-0.015}$
$\ln(\rho_{\text{re}}/M_{\text{Pl}}^4)$ (at 95% CL)	–	–	> -123	> -121
w_{re} (at 95% CL)	–	–	> -0.20	> -0.17
α^{T} (at 95% CL)	< 8.9	< 9.8	< 7.4	< 6.5
$n_{s, 0.05}$	$0.9636^{+0.0019}_{-0.0016}$	$0.9636^{+0.0016}_{-0.0011}$	$0.9633^{+0.0014}_{-0.0007}$	$0.9630^{+0.0015}_{-0.0006}$
$r_{0.05}$ (at 95% CL)	< 0.025	< 0.028	< 0.024	< 0.022
$N_{0.05}$	$52.7^{+2.5}_{-1.3}$	$53.3^{+2.1}_{-1.0}$	$53.5^{+2.0}_{-1.0}$	$53.4^{+2.2}_{-1.1}$
$\log(T_{\text{re}}/\text{GeV})$ (at 95% CL)	–	–	> 4.4	> 4.6

Parameter	E-model $_{1/2}$	E-model $_{2/3}$	E-model $_1$	E-model $_{3/2}$
$\ln(10^{10} A_s)$	3.051 ± 0.014	3.052 ± 0.014	3.051 ± 0.014	3.048 ± 0.013
$\ln(\rho_{\text{re}}/M_{\text{Pl}}^4)$ (at 95% CL)	–	–	–	–
w_{re} (at 95% CL)	–	> -0.19	> -0.21	> -0.23
α^{E} (at 95% CL)	< 36.6	< 25.4	< 18.5	< 14.6
$n_{s, 0.05}$	$0.9663^{+0.0031}_{-0.0024}$	$0.9655^{+0.0027}_{-0.0019}$	$0.9634^{+0.0026}_{-0.0020}$	$0.9624^{+0.0029}_{-0.0017}$
$r_{0.05}$ (at 95% CL)	$0.017^{+0.018}_{-0.016}$	$0.017^{+0.018}_{-0.016}$	$0.018^{+0.020}_{-0.017}$	$0.018^{+0.018}_{-0.016}$
$N_{0.05}$	$51.1^{+3.4}_{-2.6}$	$51.9^{+3.4}_{-2.1}$	$51.3^{+3.4}_{-2.7}$	$52.1^{+3.7}_{-2.1}$
$\log(T_{\text{re}}/\text{GeV})$ (at 95% CL)	–	–	–	–

Parameter	KKLT $_3$	KKLT $_5$	KKLT $_6$
$\ln(10^{10} A_s)$	3.059 ± 0.015	3.055 ± 0.015	$3.055^{+0.012}_{-0.014}$
$\ln(\rho_{\text{re}}/M_{\text{Pl}}^4)$ (at 95% CL)	–	–	< -49
w_{re} (at 95% CL)	–	–	–
$m [M_{\text{Pl}}]$ (at 95% CL)	< 5.8	< 4.9	< 6.2
$n_{s, 0.05}$	$0.9648^{+0.0049}_{-0.0019}$	$0.9675^{+0.0051}_{-0.0020}$	$0.9723^{+0.0037}_{-0.0014}$
$r_{0.05}$ (at 95% CL)	< 0.012	< 0.023	< 0.029
$N_{0.05}$	48^{+7}_{-3}	48^{+7}_{-3}	49^{+6}_{-3}
$\log(T_{\text{re}}/\text{GeV})$ (at 95% CL)	–	–	< 12.4

Table 4. Same as Table 3 for the restrictive reheating scenario.

A Additional tables

We collect constraints and mean values on the sampled and derived inflationary parameters for the restrictive reheating scenario in Table 4 and for the permissive one in Table 5.

Parameter	Λ CDM+ r	$R + R^2$	GL	Poincaré $_{7/3}$
$\ln(10^{10} A_s)$	$3.048^{+0.012}_{-0.014}$	$3.051^{+0.012}_{-0.014}$	3.055 ± 0.015	3.053 ± 0.014
$\ln(\rho_{\text{re}}/M_{\text{Pl}}^4)$ (at 95% CL)	–	–	–	–
w_{re}	–	> 0.068	> 0.044	> -0.090
$n_{\text{s}, 0.05}$	0.9672 ± 0.0035	$0.9667^{+0.0021}_{-0.0017}$	$0.9582^{+0.0042}_{-0.0038}$	$0.9607^{+0.0037}_{-0.0023}$
$r_{0.05}$ (at 95% CL)	< 0.036	0.0032 ± 0.0008	$0.0056^{+0.0015}_{-0.0014}$	$0.0088^{+0.0025}_{-0.0020}$
$N_{0.05}$	–	57.5 ± 3.7	48.3 ± 4.0	$49.7^{+4.6}_{-3.4}$
$\log(T_{\text{re}}/\text{GeV})$ (at 95% CL)	–	–	–	–

Parameter	T-model $_{1/2}$	T-model $_{2/3}$	T-model $_1$	T-model $_{3/2}$
$\ln(10^{10} A_s)$	3.053 ± 0.015	$3.050^{+0.012}_{-0.014}$	3.053 ± 0.014	3.051 ± 0.012
$\ln(\rho_{\text{re}}/M_{\text{Pl}}^4)$ (at 95% CL)	–	–	> -123	> -121
w_{re} (at 95% CL)	> -0.0019	> 0.060	> 0.041	> -0.0014
α^{T} (at 95% CL)	< 12.3	< 11.1	< 9.6	< 9.6
$n_{\text{s}, 0.05}$	$0.9665^{+0.0020}_{-0.0024}$	0.9661 ± 0.0020	$0.9657^{+0.0017}_{-0.0020}$	0.9659 ± 0.0022
$r_{0.05}$ (at 95% CL)	< 0.027	< 0.027	< 0.026	< 0.026
$N_{0.05}$	$57.1^{+2.7}_{-3.6}$	$57.4^{+2.9}_{-3.2}$	$57.6^{+2.6}_{-3.6}$	$58.4^{+3.6}_{-4.5}$
$\log(T_{\text{re}}/\text{GeV})$ (at 95% CL)	–	–	–	–

Parameter	E-model $_{1/2}$	E-model $_{2/3}$	E-model $_1$	E-model $_{3/2}$
$\ln(10^{10} A_s)$	$3.055^{+0.013}_{-0.014}$	3.058 ± 0.013	3.055 ± 0.014	3.053 ± 0.014
$\ln(\rho_{\text{re}}/M_{\text{Pl}}^4)$ (at 95% CL)	–	–	–	–
w_{re} (at 95% CL)	-0.068	> 0.024	> -0.036	> 0.037
α^{E} (at 95% CL)	< 26.3	< 21.7	< 22.1	< 16.1
$n_{\text{s}, 0.05}$	$0.9628^{+0.0052}_{-0.0034}$	$0.9609^{+0.0059}_{-0.0037}$	$0.9616^{+0.0044}_{-0.0029}$	$0.9602^{+0.0040}_{-0.0030}$
$r_{0.05}$ (at 95% CL)	< 0.034	< 0.034	< 0.042	$0.020^{+0.022}_{-0.020}$
$N_{0.05}$	$48.5^{+4.0}_{-4.7}$	$48.1^{+3.7}_{-4.9}$	$49.4^{+4.8}_{-3.6}$	49.4 ± 3.8
$\log(T_{\text{re}}/\text{GeV})$ (at 95% CL)	–	–	–	–

Parameter	KKLT $_3$	KKLT $_5$	KKLT $_6$
$\ln(10^{10} A_s)$	3.052 ± 0.015	3.053 ± 0.014	3.052 ± 0.016
$\ln(\rho_{\text{re}}/M_{\text{Pl}}^4)$ (at 95% CL)	–	–	< -64.5
w_{re} (at 95% CL)	–	–	–
$m [M_{\text{Pl}}]$ (at 95% CL)	< 6.3	< 4.5	< 4.9
$n_{\text{s}, 0.05}$	$0.9679^{+0.0048}_{-0.0021}$	$0.9696^{+0.0066}_{-0.0026}$	$0.9730^{+0.0074}_{-0.0027}$
$r_{0.05}$ (at 95% CL)	< 0.012	< 0.019	< 0.025
$N_{0.05}$	54^{+7}_{-4}	52^{+10}_{-5}	53^{+10}_{-6}
$\log(T_{\text{re}}/\text{GeV})$ (at 95% CL)	–	–	< 10.8

Table 5. Same as Table 3 for the permissive reheating scenario.

References

- [1] A.A. Starobinsky, *A new type of isotropic cosmological models without singularity*, *Physics Letters B* **91** (1980) 99.
- [2] A.H. Guth, *Inflationary universe: A possible solution to the horizon and flatness problems*, *Phys. Rev. D* **23** (1981) 347.
- [3] A.D. Linde, *A new inflationary universe scenario: A possible solution of the horizon, flatness, homogeneity, isotropy and primordial monopole problems*, *Physics Letters B* **108** (1982) 389.
- [4] A. Albrecht and P.J. Steinhardt, *Cosmology for Grand Unified Theories with Radiatively Induced Symmetry Breaking*, *Phys. Rev. Lett.* **48** (1982) 1220.
- [5] S.W. Hawking, I.G. Moss and J.M. Stewart, *Bubble collisions in the very early universe*, *Phys. Rev. D* **26** (1982) 2681.
- [6] A.D. Linde, *Chaotic inflation*, *Physics Letters B* **129** (1983) 177.
- [7] Planck Collaboration, P.A.R. Ade, N. Aghanim, C. Armitage-Caplan, M. Arnaud, M. Ashdown et al., *Planck 2013 results. XXII. Constraints on inflation*, *A&A* **571** (2014) A22 [[1303.5082](#)].
- [8] Planck Collaboration, P.A.R. Ade, N. Aghanim, C. Armitage-Caplan, M. Arnaud, M. Ashdown et al., *Planck 2013 results. XXIV. Constraints on primordial non-Gaussianity*, *A&A* **571** (2014) A24 [[1303.5084](#)].
- [9] Planck Collaboration, P.A.R. Ade, N. Aghanim, M. Arnaud, F. Arroja, M. Ashdown et al., *Planck 2015 results. XX. Constraints on inflation*, *A&A* **594** (2016) A20 [[1502.02114](#)].
- [10] Planck Collaboration, P.A.R. Ade, N. Aghanim, M. Arnaud, F. Arroja, M. Ashdown et al., *Planck 2015 results. XVII. Constraints on primordial non-Gaussianity*, *A&A* **594** (2016) A17 [[1502.01592](#)].
- [11] Planck Collaboration, Y. Akrami, F. Arroja, M. Ashdown, J. Aumont, C. Baccigalupi et al., *Planck 2018 results. X. Constraints on inflation*, *A&A* **641** (2020) A10 [[1807.06211](#)].
- [12] Planck Collaboration, Y. Akrami, F. Arroja, M. Ashdown, J. Aumont, C. Baccigalupi et al., *Planck 2018 results. IX. Constraints on primordial non-Gaussianity*, *A&A* **641** (2020) A9 [[1905.05697](#)].
- [13] M. Kamionkowski, A. Kosowsky and A. Stebbins, *Statistics of cosmic microwave background polarization*, *Phys. Rev. D* **55** (1997) 7368 [[astro-ph/9611125](#)].
- [14] M. Kamionkowski, A. Kosowsky and A. Stebbins, *A Probe of Primordial Gravity Waves and Vorticity*, *Phys. Rev. Lett.* **78** (1997) 2058 [[astro-ph/9609132](#)].
- [15] U. Seljak and M. Zaldarriaga, *Signature of Gravity Waves in the Polarization of the Microwave Background*, *Phys. Rev. Lett.* **78** (1997) 2054 [[astro-ph/9609169](#)].
- [16] M. Zaldarriaga and U. Seljak, *All-sky analysis of polarization in the microwave background*, *Phys. Rev. D* **55** (1997) 1830 [[astro-ph/9609170](#)].

- [17] U. Seljak, *Measuring Polarization in the Cosmic Microwave Background*, *ApJ* **482** (1997) 6 [[astro-ph/9608131](#)].
- [18] A.A. Starobinskiĭ, *Spectrum of relict gravitational radiation and the early state of the universe*, *Soviet Journal of Experimental and Theoretical Physics Letters* **30** (1979) 682.
- [19] V.A. Rubakov, M.V. Sazhin and A.V. Veryaskin, *Graviton creation in the inflationary universe and the grand unification scale*, *Physics Letters B* **115** (1982) 189.
- [20] R. Fabbri and M.D. Pollock, *The effect of primordially produced gravitons upon the anisotropy of the cosmological microwave background radiation*, *Physics Letters B* **125** (1983) 445.
- [21] L. Abbott and M.B. Wise, *Constraints on generalized inflationary cosmologies*, *Nuclear Physics B* **244** (1984) 541.
- [22] M. Kamionkowski and A. Kosowsky, *The Cosmic Microwave Background and Particle Physics*, *Annual Review of Nuclear and Particle Science* **49** (1999) 77 [[astro-ph/9904108](#)].
- [23] M. Kamionkowski and E.D. Kovetz, *The Quest for B Modes from Inflationary Gravitational Waves*, *ARA&A* **54** (2016) 227 [[1510.06042](#)].
- [24] P. Ade, J. Aguirre, Z. Ahmed, S. Aiola, A. Ali, D. Alonso et al., *The Simons Observatory: science goals and forecasts*, *J. Cosmology Astropart. Phys.* **2019** (2019) 056 [[1808.07445](#)].
- [25] K. Abazajian, G.E. Addison, P. Adshead, Z. Ahmed, D. Akerib, A. Ali et al., *CMB-S4: Forecasting Constraints on Primordial Gravitational Waves*, *ApJ* **926** (2022) 54 [[2008.12619](#)].
- [26] LiteBIRD Collaboration, E. Allys, K. Arnold, J. Aumont, R. Aurlieu, S. Azzoni et al., *Probing cosmic inflation with the LiteBIRD cosmic microwave background polarization survey*, *Progress of Theoretical and Experimental Physics* **2023** (2023) 042F01 [[2202.02773](#)].
- [27] S. Dodelson and L. Hui, *Horizon Ratio Bound for Inflationary Fluctuations*, *Phys. Rev. Lett.* **91** (2003) 131301 [[astro-ph/0305113](#)].
- [28] A.R. Liddle and S.M. Leach, *How long before the end of inflation were observable perturbations produced?*, *Phys. Rev. D* **68** (2003) 103503 [[astro-ph/0305263](#)].
- [29] W.H. Kinney and A. Riotto, *Theoretical uncertainties in inflationary predictions*, *J. Cosmology Astropart. Phys.* **2006** (2006) 011 [[astro-ph/0511127](#)].
- [30] J. Martin and C. Ringeval, *Inflation after WMAP3: confronting the slow-roll and exact power spectra with CMB data*, *J. Cosmology Astropart. Phys.* **2006** (2006) 009 [[astro-ph/0605367](#)].
- [31] P. Adshead, R. Easther, J. Pritchard and A. Loeb, *Inflation and the scale dependent spectral index: prospects and strategies*, *J. Cosmology Astropart. Phys.* **2011** (2011) 021 [[1007.3748](#)].
- [32] M.J. Mortonson, H.V. Peiris and R. Easther, *Bayesian analysis of inflation: Parameter estimation for single field models*, *Phys. Rev. D* **83** (2011) 043505 [[1007.4205](#)].

- [33] R. Allahverdi, R. Brandenberger, F.-Y. Cyr-Racine and A. Mazumdar, *Reheating in Inflationary Cosmology: Theory and Applications*, *Annual Review of Nuclear and Particle Science* **60** (2010) 27 [[1001.2600](#)].
- [34] J. Martin and C. Ringeval, *First CMB constraints on the inflationary reheating temperature*, *Phys. Rev. D* **82** (2010) 023511 [[1004.5525](#)].
- [35] J. Martin, C. Ringeval and R. Trotta, *Hunting down the best model of inflation with Bayesian evidence*, *Phys. Rev. D* **83** (2011) 063524 [[1009.4157](#)].
- [36] R. Easther and H.V. Peiris, *Bayesian analysis of inflation. II. Model selection and constraints on reheating*, *Phys. Rev. D* **85** (2012) 103533 [[1112.0326](#)].
- [37] J. Martin, C. Ringeval, R. Trotta and V. Vennin, *The best inflationary models after Planck*, *J. Cosmology Astropart. Phys.* **2014** (2014) 039 [[1312.3529](#)].
- [38] J. Martin, C. Ringeval and V. Vennin, *Observing Inflationary Reheating*, *Phys. Rev. Lett.* **114** (2015) 081303 [[1410.7958](#)].
- [39] J. Martin, C. Ringeval and V. Vennin, *How well can future CMB missions constrain cosmic inflation?*, *J. Cosmology Astropart. Phys.* **2014** (2014) 038 [[1407.4034](#)].
- [40] L. Dai, M. Kamionkowski and J. Wang, *Reheating Constraints to Inflationary Models*, *Phys. Rev. Lett.* **113** (2014) 041302 [[1404.6704](#)].
- [41] J.B. Muñoz and M. Kamionkowski, *Equation-of-state parameter for reheating*, *Phys. Rev. D* **91** (2015) 043521 [[1412.0656](#)].
- [42] J.L. Cook, E. Dimastrogiovanni, D.A. Easson and L.M. Krauss, *Reheating predictions in single field inflation*, *J. Cosmology Astropart. Phys.* **2015** (2015) 047 [[1502.04673](#)].
- [43] Y. Ueno and K. Yamamoto, *Constraints on α -attractor inflation and reheating*, *Phys. Rev. D* **93** (2016) 083524 [[1602.07427](#)].
- [44] L.T. Hergt, W.J. Handley, M.P. Hobson and A.N. Lasenby, *Constraining the kinetically dominated universe*, *Phys. Rev. D* **100** (2019) 023501 [[1809.07737](#)].
- [45] J. Ellis, M.A.G. Garcia, D.V. Nanopoulos, K.A. Olive and S. Verner, *BICEP/Keck constraints on attractor models of inflation and reheating*, *Phys. Rev. D* **105** (2022) 043504 [[2112.04466](#)].
- [46] L.T. Hergt, F.J. Agocs, W.J. Handley, M.P. Hobson and A.N. Lasenby, *Finite inflation in curved space*, *Phys. Rev. D* **106** (2022) 063529 [[2205.07374](#)].
- [47] P.A.R. Ade, Z. Ahmed, M. Amiri, D. Barkats, R.B. Thakur, C.A. Bischoff et al., *Improved Constraints on Primordial Gravitational Waves using Planck, WMAP, and BICEP/Keck Observations through the 2018 Observing Season*, *Phys. Rev. Lett.* **127** (2021) 151301 [[2110.00483](#)].
- [48] V.F. Mukhanov and G.V. Chibisov, *Quantum fluctuations and a nonsingular universe*, *Soviet Journal of Experimental and Theoretical Physics Letters* **33** (1981) 532.
- [49] J. Martin, C. Ringeval and V. Vennin, *Encyclopædia Inflationaris*, *Physics of the Dark Universe* **5** (2014) 75 [[1303.3787](#)].
- [50] J. Martin, C. Ringeval and V. Vennin, *Cosmic Inflation at the Crossroads*, *arXiv e-prints* (2024) [arXiv:2404.10647](#) [[2404.10647](#)].

- [51] V.F. Mukhanov, *Gravitational instability of the universe filled with a scalar field*, *Soviet Journal of Experimental and Theoretical Physics Letters* **41** (1985) 493.
- [52] V.F. Mukhanov, *Quantum theory of gauge-invariant cosmological perturbations*, *Soviet Journal of Experimental and Theoretical Physics* **67** (1988) 1297.
- [53] E.D. Stewart and D.H. Lyth, *A more accurate analytic calculation of the spectrum of cosmological perturbations produced during inflation*, *Physics Letters B* **302** (1993) 171 [[gr-qc/9302019](#)].
- [54] A.R. Liddle, P. Parsons and J.D. Barrow, *Formalizing the slow-roll approximation in inflation*, *Phys. Rev. D* **50** (1994) 7222 [[astro-ph/9408015](#)].
- [55] E.D. Stewart and J.O. Gong, *The density perturbation power spectrum to second-order corrections in the slow-roll expansion*, *Physics Letters B* **510** (2001) 1 [[astro-ph/0101225](#)].
- [56] D.J. Schwarz, C.A. Terrero-Escalante and A.A. García, *Higher order corrections to primordial spectra from cosmological inflation*, *Physics Letters B* **517** (2001) 243 [[astro-ph/0106020](#)].
- [57] S.M. Leach, A.R. Liddle, J. Martin and D.J. Schwarz, *Cosmological parameter estimation and the inflationary cosmology*, *Phys. Rev. D* **66** (2002) 023515 [[astro-ph/0202094](#)].
- [58] P. Auclair and C. Ringeval, *Slow-roll inflation at N³LO*, *Phys. Rev. D* **106** (2022) 063512 [[2205.12608](#)].
- [59] E. Bianchi and M. Gamonal, *Primordial power spectrum at N³LO in effective theories of inflation*, *arXiv e-prints* (2024) [arXiv:2405.03157](#) [[2405.03157](#)].
- [60] J. Froustey, C. Pitrou and M.C. Volpe, *Neutrino decoupling including flavour oscillations and primordial nucleosynthesis*, *J. Cosmology Astropart. Phys.* **2020** (2020) 015 [[2008.01074](#)].
- [61] D.J. Fixsen, *The Temperature of the Cosmic Microwave Background*, *ApJ* **707** (2009) 916 [[0911.1955](#)].
- [62] Planck Collaboration, N. Aghanim, Y. Akrami, M. Ashdown, J. Aumont, C. Baccigalupi et al., *Planck 2018 results. VI. Cosmological parameters*, *A&A* **641** (2020) A6 [[1807.06209](#)].
- [63] A.A. Starobinskii, *The Perturbation Spectrum Evolving from a Nonsingular Initially De-Sitter Cosmology and the Microwave Background Anisotropy*, *Soviet Astronomy Letters* **9** (1983) 302.
- [64] F. Bezrukov and M. Shaposhnikov, *The Standard Model Higgs boson as the inflaton*, *Physics Letters B* **659** (2008) 703 [[0710.3755](#)].
- [65] D.S. Gorbunov and A.G. Panin, *Scalaron the mighty: Producing dark matter and baryon asymmetry at reheating*, *Physics Letters B* **700** (2011) 157 [[1009.2448](#)].
- [66] F.L. Bezrukov and D.S. Gorbunov, *Distinguishing between R²-inflation and Higgs-inflation*, *Physics Letters B* **713** (2012) 365 [[1111.4397](#)].
- [67] A. Vilenkin, *Classical and quantum cosmology of the Starobinsky inflationary model*, *Phys. Rev. D* **32** (1985) 2511.

- [68] R. Kallosh, A. Linde and D. Roest, *Universal Attractor for Inflation at Strong Coupling*, *Phys. Rev. Lett.* **112** (2014) 011303 [[1310.3950](#)].
- [69] S. Ferrara, R. Kallosh, A. Linde and M. Porrati, *Minimal supergravity models of inflation*, *Phys. Rev. D* **88** (2013) 085038 [[1307.7696](#)].
- [70] R. Kallosh, A. Linde and D. Roest, *Superconformal inflationary α -attractors*, *Journal of High Energy Physics* **2013** (2013) 198 [[1311.0472](#)].
- [71] R. Kallosh, A. Linde and D. Roest, *Large field inflation and double α -attractors*, *Journal of High Energy Physics* **2014** (2014) 52 [[1405.3646](#)].
- [72] R. Kallosh, A. Linde and D. Roest, *The double attractor behavior of induced inflation*, *Journal of High Energy Physics* **2014** (2014) 62 [[1407.4471](#)].
- [73] M. Galante, R. Kallosh, A. Linde and D. Roest, *Unity of Cosmological Inflation Attractors*, *Phys. Rev. Lett.* **114** (2015) 141302.
- [74] R. Kallosh and A. Linde, *Universality class in conformal inflation*, *J. Cosmology Astropart. Phys.* **2013** (2013) 002 [[1306.5220](#)].
- [75] J.J.M. Carrasco, R. Kallosh, A. Linde and D. Roest, *Hyperbolic geometry of cosmological attractors*, *Phys. Rev. D* **92** (2015) 041301 [[1504.05557](#)].
- [76] R. Kallosh and A. Linde, *Superconformal generalization of the chaotic inflation model*, *J. Cosmology Astropart. Phys.* **2013** (2013) 027 [[1306.3211](#)].
- [77] A.S. Goncharov and A.D. Linde, *Chaotic inflation in supergravity*, *Physics Letters B* **139** (1984) 27.
- [78] M. Cicoli, C.P. Burgess and F. Quevedo, *Fibre inflation: observable gravity waves from IIB string compactifications*, *J. Cosmology Astropart. Phys.* **2009** (2009) 013 [[0808.0691](#)].
- [79] R. Kallosh, A. Linde, D. Roest, A. Westphal and Y. Yamada, *Fibre inflation and α -attractors*, *Journal of High Energy Physics* **2018** (2018) 117 [[1707.05830](#)].
- [80] S. Kachru, R. Kallosh, A. Linde, J. Maldacena, L. McAllister and S.P. Trivedi, *Towards inflation in string theory*, *J. Cosmology Astropart. Phys.* **2003** (2003) 013 [[hep-th/0308055](#)].
- [81] G. Dvali, Q. Shafi and S. Solganik, *D-brane Inflation*, pp. hep-th/0105203, May, 2001, DOI [[hep-th/0105203](#)].
- [82] C.P. Burgess, M. Majumdar, D. Nolte, F. Quevedo, G. Rajesh and R.-J. Zhang, *The inflationary brane-antibrane universe*, *Journal of High Energy Physics* **2001** (2001) 047 [[hep-th/0105204](#)].
- [83] J. García-Bellido, R. Rabadán and F. Zamora, *Inflationary scenarios from branes at angles*, *Journal of High Energy Physics* **2002** (2002) 036 [[hep-th/0112147](#)].
- [84] S. Kachru, R. Kallosh, A. Linde and S.P. Trivedi, *de Sitter vacua in string theory*, *Phys. Rev. D* **68** (2003) 046005 [[hep-th/0301240](#)].
- [85] R. Kallosh, A. Linde and Y. Yamada, *Planck 2018 and brane inflation revisited*, *Journal of High Energy Physics* **2019** (2019) 8 [[1811.01023](#)].
- [86] R. Kallosh and A. Linde, *On hilltop and brane inflation after Planck*, *J. Cosmology Astropart. Phys.* **2019** (2019) 030 [[1906.02156](#)].

- [87] V. Balasubramanian, P. Berglund, J.P. Conlon and F. Quevedo, *Systematics of Moduli Stabilisation in Calabi-Yau Flux Compactifications*, *Journal of High Energy Physics* **2005** (2005) 007 [[hep-th/0502058](#)].
- [88] J.P. Conlon, F. Quevedo and K. Suruliz, *Large-volume flux compactifications: moduli spectrum and D3/D7 soft supersymmetry breaking*, *Journal of High Energy Physics* **2005** (2005) 007 [[hep-th/0505076](#)].
- [89] R. Kallosh and T. Wrase, *dS Supergravity from 10d*, *Fortschritte der Physik* **67** (2019) 1800071 [[1808.09427](#)].
- [90] J. Blåbäck, U. Danielsson and G. Dibitetto, *A new light on the darkest corner of the landscape*, *arXiv e-prints* (2018) arXiv:1810.11365 [[1810.11365](#)].
- [91] A. Lewis, *Efficient sampling of fast and slow cosmological parameters*, *Phys. Rev. D* **87** (2013) 103529 [[1304.4473](#)].
- [92] A. Lewis, A. Challinor and A. Lasenby, *Efficient Computation of Cosmic Microwave Background Anisotropies in Closed Friedmann-Robertson-Walker Models*, *ApJ* **538** (2000) 473 [[astro-ph/9911177](#)].
- [93] C. Howlett, A. Lewis, A. Hall and A. Challinor, *CMB power spectrum parameter degeneracies in the era of precision cosmology*, *J. Cosmology Astropart. Phys.* **2012** (2012) 027 [[1201.3654](#)].
- [94] W.J. Handley, M.P. Hobson and A.N. Lasenby, *polychord: nested sampling for cosmology.*, *MNRAS* **450** (2015) L61 [[1502.01856](#)].
- [95] W.J. Handley, M.P. Hobson and A.N. Lasenby, *POLYCHORD: next-generation nested sampling*, *MNRAS* **453** (2015) 4384 [[1506.00171](#)].
- [96] A. Lewis, *GetDist: a Python package for analysing Monte Carlo samples*, *arXiv e-prints* (2019) arXiv:1910.13970 [[1910.13970](#)].
- [97] W. Handley, *anesthetic: nested sampling visualisation*, *The Journal of Open Source Software* **4** (2019) 1414 [[1905.04768](#)].
- [98] Planck Collaboration, N. Aghanim, Y. Akrami, M. Ashdown, J. Aumont, C. Baccigalupi et al., *Planck 2018 results. V. CMB power spectra and likelihoods*, *A&A* **641** (2020) A5 [[1907.12875](#)].
- [99] S. Alam, M. Aubert, S. Avila, C. Balland, J.E. Bautista, M.A. Bershadsky et al., *Completed SDSS-IV extended Baryon Oscillation Spectroscopic Survey: Cosmological implications from two decades of spectroscopic surveys at the Apache Point Observatory*, *Phys. Rev. D* **103** (2021) 083533 [[2007.08991](#)].
- [100] D.M. Scolnic, D.O. Jones, A. Rest, Y.C. Pan, R. Chornock, R.J. Foley et al., *The Complete Light-curve Sample of Spectroscopically Confirmed SNe Ia from Pan-STARRS1 and Cosmological Constraints from the Combined Pantheon Sample*, *ApJ* **859** (2018) 101 [[1710.00845](#)].
- [101] M.S. Turner, *Coherent scalar-field oscillations in an expanding universe*, *Phys. Rev. D* **28** (1983) 1243.
- [102] A. Linde, *Does the first chaotic inflation model in supergravity provide the best fit to the Planck data?*, *J. Cosmology Astropart. Phys.* **2015** (2015) 030 [[1412.7111](#)].

- [103] S. Ferrara and R. Kallosh, *Seven-disk manifold, α -attractors, and B modes*, *Phys. Rev. D* **94** (2016) 126015 [[1610.04163](#)].
- [104] R. Kallosh and A. Linde, *CMB targets after the latest Planck data release*, *Phys. Rev. D* **100** (2019) 123523 [[1909.04687](#)].
- [105] R.E. Kass and A.E. Raftery, *Bayes factors*, *J. Amer. Statist. Assoc.* **90** (1995) 773.
- [106] L.T. Hergt, W.J. Handley, M.P. Hobson and A.N. Lasenby, *Bayesian evidence for the tensor-to-scalar ratio r and neutrino masses m_ν : Effects of uniform vs logarithmic priors*, *Phys. Rev. D* **103** (2021) 123511 [[2102.11511](#)].
- [107] P.F. de Salas, M. Lattanzi, G. Mangano, G. Miele, S. Pastor and O. Pisanti, *Bounds on very low reheating scenarios after Planck*, *Phys. Rev. D* **92** (2015) 123534 [[1511.00672](#)].
- [108] C. Pallis, *Kination-dominated reheating and cold dark matter abundance*, *Nuclear Physics B* **751** (2006) 129 [[hep-ph/0510234](#)].
- [109] J. Ellis, A.D. Linde and D.V. Nanopoulos, *Inflation can save the gravitino*, *Physics Letters B* **118** (1982) 59.
- [110] M. Tristram, A.J. Banday, K.M. Górski, R. Keskitalo, C.R. Lawrence, K.J. Andersen et al., *Improved limits on the tensor-to-scalar ratio using BICEP and Planck data*, *Phys. Rev. D* **105** (2022) 083524 [[2112.07961](#)].
- [111] G. Galloni, N. Bartolo, S. Matarrese, M. Migliaccio, A. Ricciardone and N. Vittorio, *Updated constraints on amplitude and tilt of the tensor primordial spectrum*, *J. Cosmology Astropart. Phys.* **2023** (2023) 062 [[2208.00188](#)].
- [112] G. Galloni, S. Henrot-Versillé and M. Tristram, *Robust constraints on tensor perturbations from cosmological data: a comparative analysis from Bayesian and frequentist perspectives*, *arXiv e-prints* (2024) arXiv:2405.04455 [[2405.04455](#)].
- [113] E. Rosenberg, S. Gratton and G. Efstathiou, *CMB power spectra and cosmological parameters from Planck PR4 with CamSpec*, *MNRAS* **517** (2022) 4620 [[2205.10869](#)].
- [114] M. Tristram, A.J. Banday, M. Douspis, X. Garrido, K.M. Górski, S. Henrot-Versillé et al., *Cosmological parameters derived from the final Planck data release (PR4)*, *A&A* **682** (2024) A37 [[2309.10034](#)].
- [115] M. Ballardini, F. Finelli, C. Fedeli and L. Moscardini, *Probing primordial features with future galaxy surveys*, *J. Cosmology Astropart. Phys.* **2016** (2016) 041 [[1606.03747](#)].
- [116] Euclid Collaboration, S. Ilić, N. Aghanim, C. Baccigalupi, J.R. Bermejo-Climent, G. Fabbian et al., *Euclid preparation. XV. Forecasting cosmological constraints for the Euclid and CMB joint analysis*, *A&A* **657** (2022) A91 [[2106.08346](#)].
- [117] Euclid Collaboration, Y. Mellier, Abdurro'uf, J.A. Acevedo Barroso, A. Achúcarro, J. Adamek et al., *Euclid. I. Overview of the Euclid mission*, *arXiv e-prints* (2024) arXiv:2405.13491 [[2405.13491](#)].
- [118] R. Kallosh and A. Linde, *BICEP/Keck and cosmological attractors*, *J. Cosmology Astropart. Phys.* **2021** (2021) 008 [[2110.10902](#)].

- [119] R. Kallosh and A. Linde, *B-mode targets*, *Physics Letters B* **798** (2019) 134970 [[1906.04729](#)].
- [120] K.D. Lozanov and M.A. Amin, *Equation of State and Duration to Radiation Domination after Inflation*, *Phys. Rev. Lett.* **119** (2017) 061301 [[1608.01213](#)].
- [121] S. Antusch, D.G. Figueroa, K. Marschall and F. Torrenti, *Energy distribution and equation of state of the early Universe: Matching the end of inflation and the onset of radiation domination*, *Physics Letters B* **811** (2020) 135888 [[2005.07563](#)].
- [122] S. Antusch, D.G. Figueroa, K. Marschall and F. Torrenti, *Characterizing the postinflationary reheating history: Single daughter field with quadratic-quadratic interaction*, *Phys. Rev. D* **105** (2022) 043532 [[2112.11280](#)].
- [123] W. Giarè, S. Pan, E. Di Valentino, W. Yang, J. de Haro and A. Melchiorri, *Inflationary potential as seen from different angles: model compatibility from multiple CMB missions*, *J. Cosmology Astropart. Phys.* **2023** (2023) 019 [[2305.15378](#)].
- [124] DESI Collaboration, A.G. Adame, J. Aguilar, S. Ahlen, S. Alam, D.M. Alexander et al., *DESI 2024 VI: Cosmological Constraints from the Measurements of Baryon Acoustic Oscillations*, *arXiv e-prints* (2024) [arXiv:2404.03002](#) [[2404.03002](#)].
- [125] D. Wang, *Constraining Cosmological Physics with DESI BAO Observations*, *arXiv e-prints* (2024) [arXiv:2404.06796](#) [[2404.06796](#)].
- [126] S. Aiola, E. Calabrese, L. Maurin, S. Naess, B.L. Schmitt, M.H. Abitbol et al., *The Atacama Cosmology Telescope: DR4 maps and cosmological parameters*, *J. Cosmology Astropart. Phys.* **2020** (2020) 047 [[2007.07288](#)].